Classification of gapless Z_2 spin liquids in three-dimensional Kitaev models

Maria Hermanns
University of Cologne

M.H., S. Trebst, PRB 89, 235102 (2014)

M.H., K. O'Brien, S. Trebst, PRL 114, 157202 (2015)

M.H., S. Trebst, A. Rosch, arXiv:1506.01379 (2015)

Emmy Noether-Programm
DFG Deutsche Forschungsgemeinschaft

Classification of gapless Z_2 spin liquids in three-dimensional Kitaev models

Maria Hermanns

University of Cologne

Kevin O'Brien

M.H., S. Trebst, PRB 89, 235102 (2014)

M.H., K. O'Brien, S. Trebst, PRL 114, 157202 (2015)

M.H., S. Trebst, A. Rosch, arXiv:1506.01379 (2015)

Emmy Noether-Programm

DFG Deutsche Forschungsgemeinschaft

A family of Li_2IrO_3 compounds

crystals

α–Li_2IrO_3	β–Li_2IrO_3	γ – Li_2IrO_3
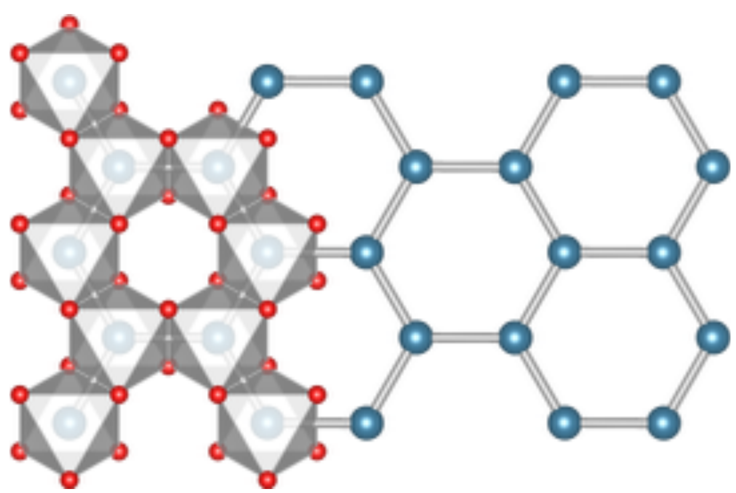	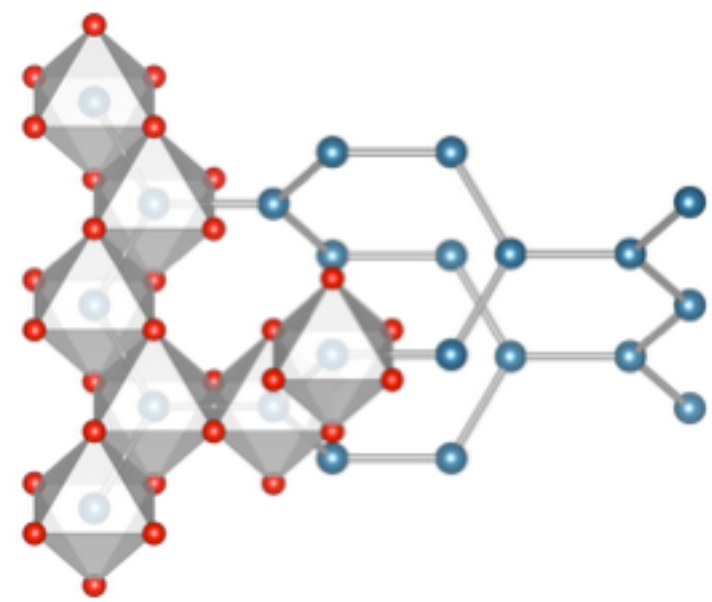	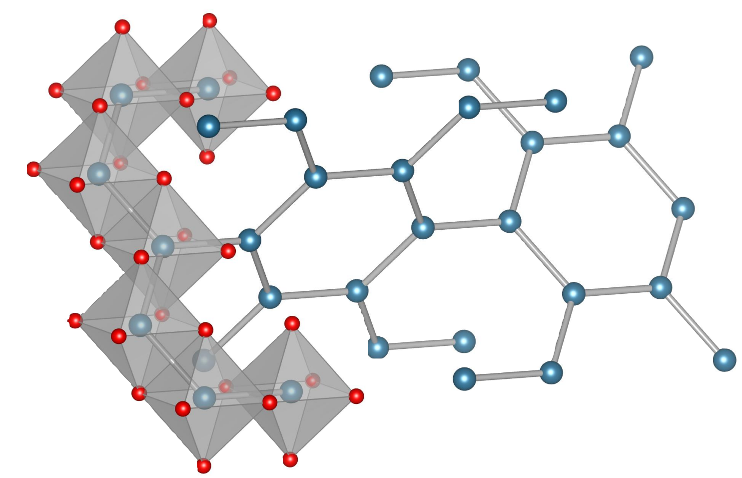
Singh et al., PRL **108**, 127203 (2008)	Takayama et al., PRL 114, 077202 (2015)	Modic et al. , Nat. Comm. 5, 4203 (2014)

edge-sharing IrO_6 octahedra

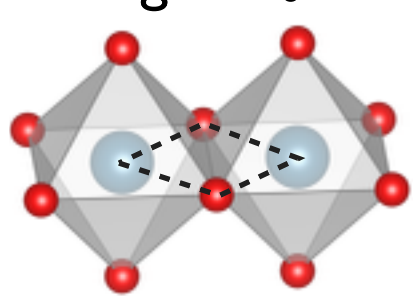

G. Jackeli and G. Khaliullin (2009)

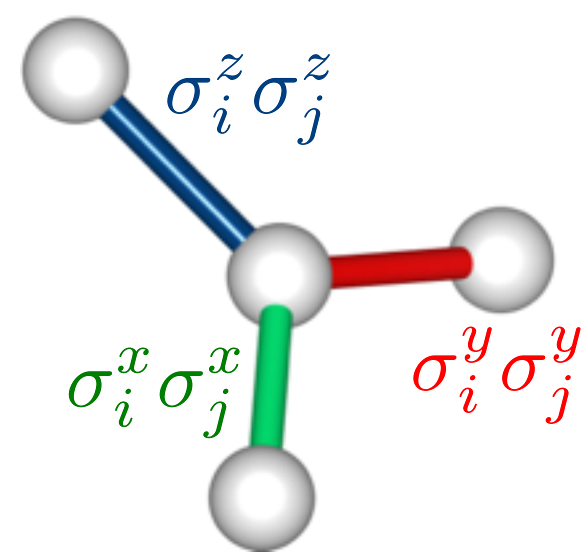

A family of Li_2IrO_3 compounds

α–Li_2IrO_3 | β–Li_2IrO_3 | $\gamma - Li_2IrO_3$

crystals

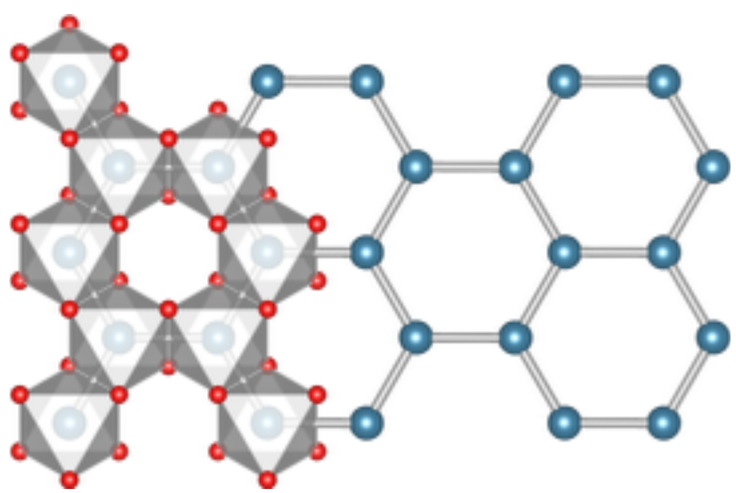

Singh et al., PRL **108**, 127203 (2008)

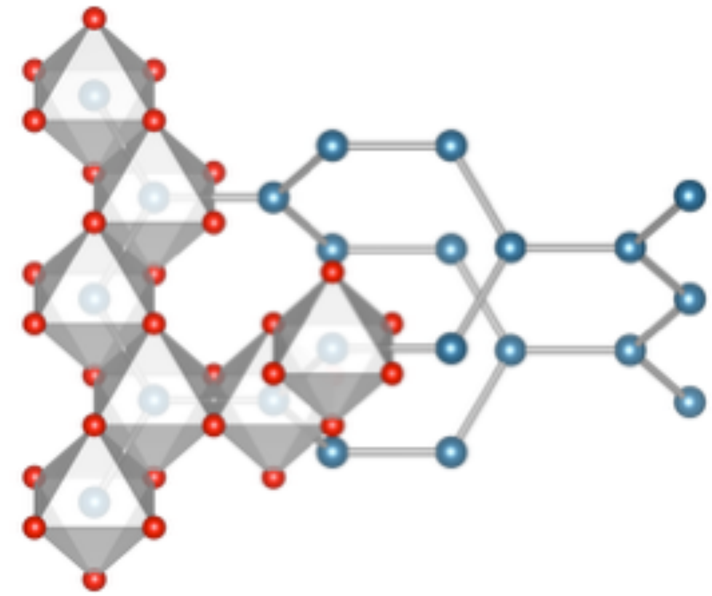

Takayama et al., PRL 114, 077202 (2015)

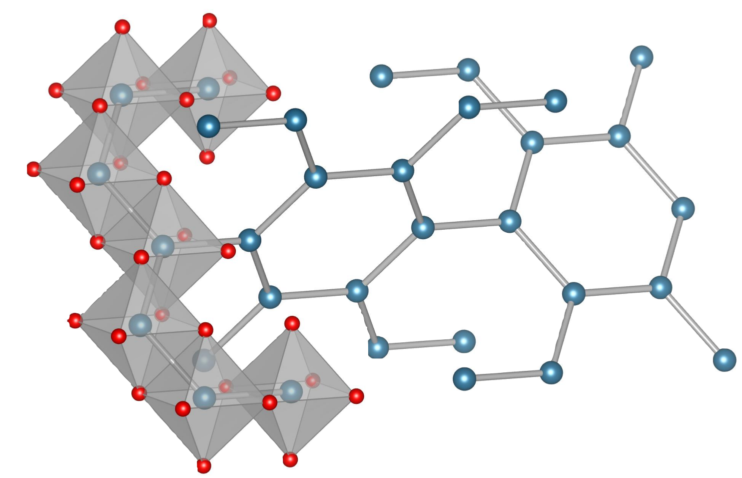

Modic et al. , Nat. Comm. 5, 4203 (2014)

Kitaev models

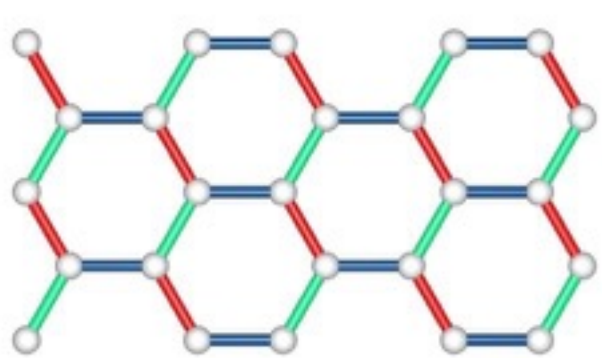

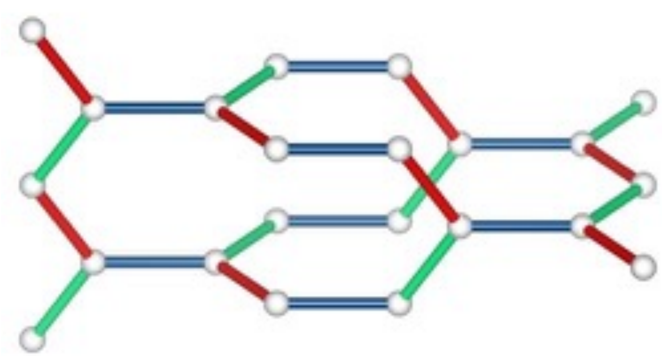

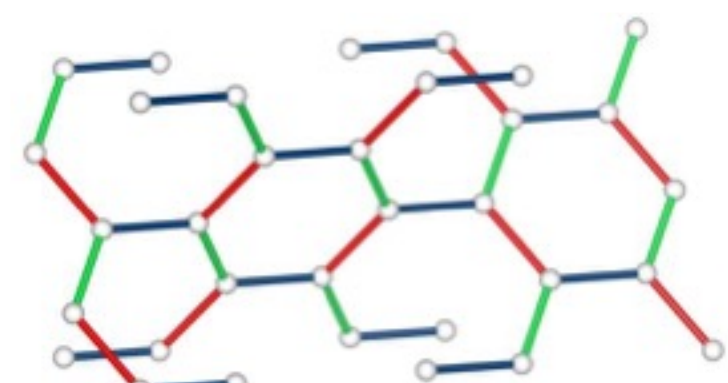

Na_2IrO_3: Singh, Gegenwart, PRB 82, 064412 (2010)
$RuCl_3$: Majumder et al. PRB 91, 180401(R) (2015)

Tricoordinated lattices in 3D

Tricoordinated lattices in 3D

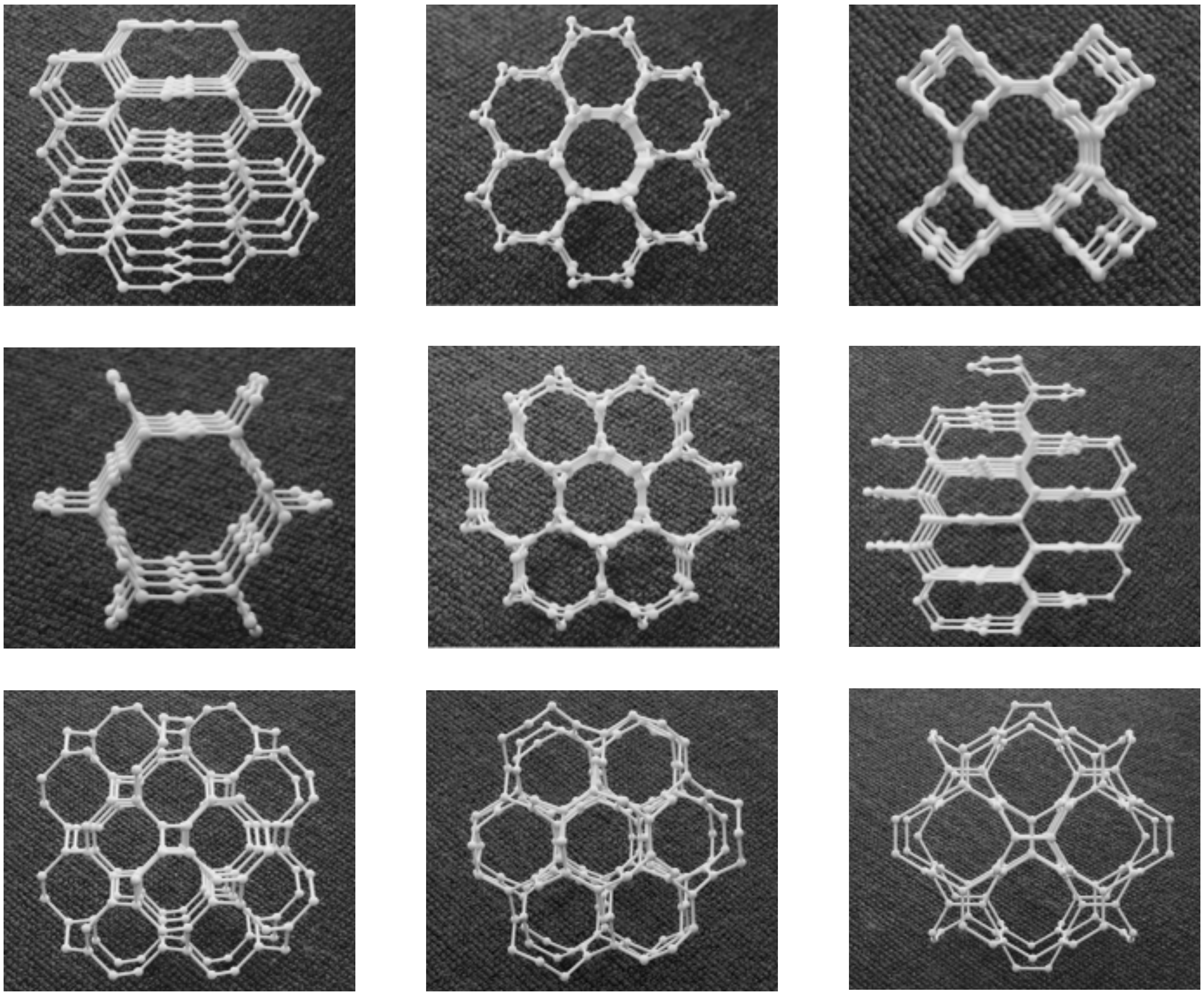

Tricoordinated lattices in 3D

(10,3)

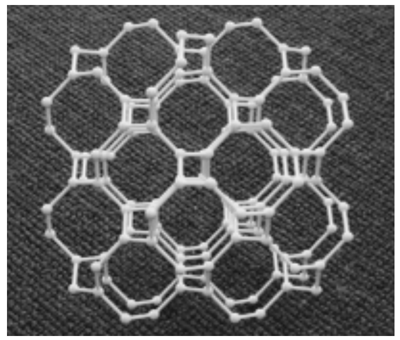
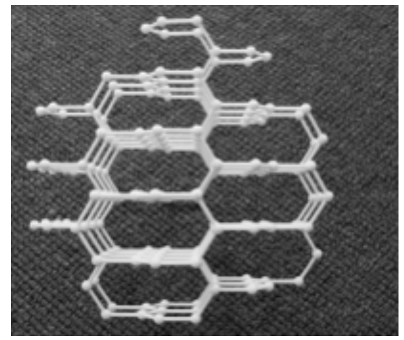
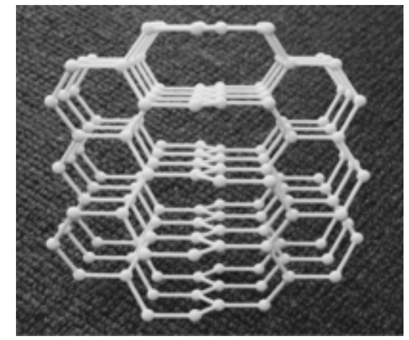

(9,3)

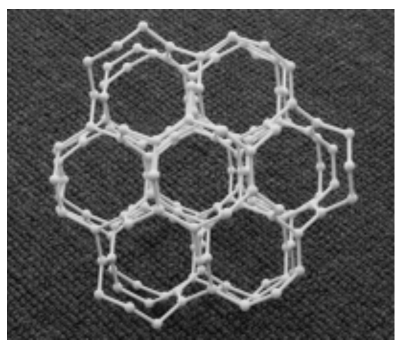
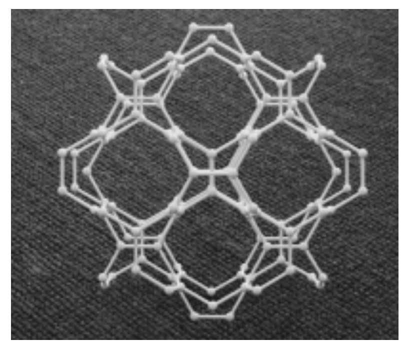

(8,3)

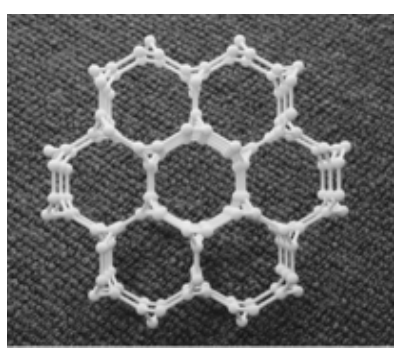
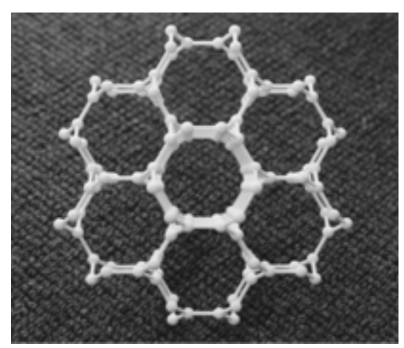
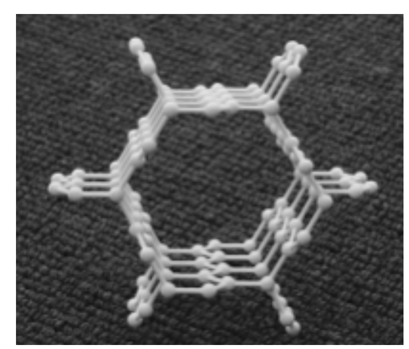
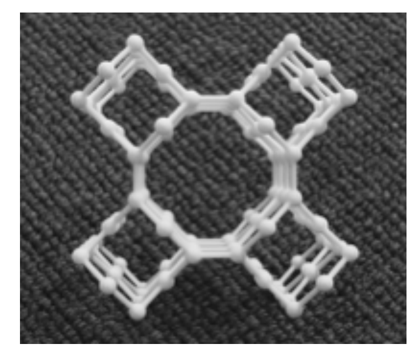

Tricoordinated lattices in 3D

(10,3)

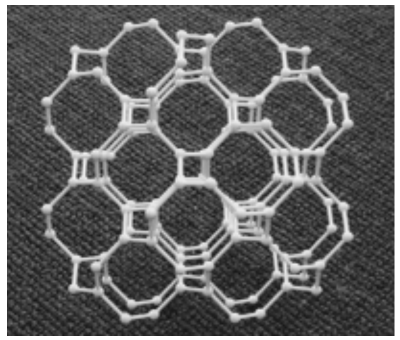
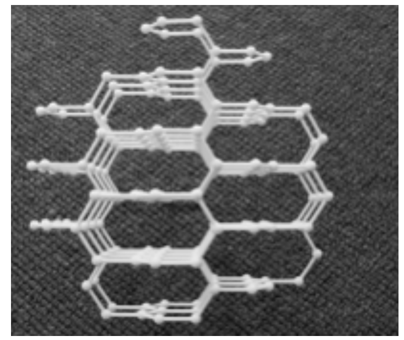
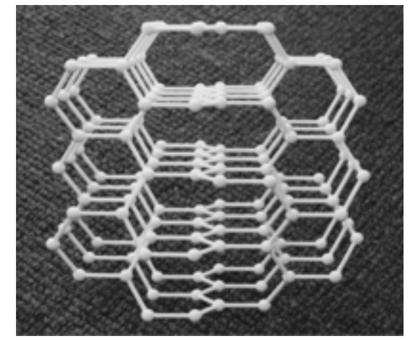

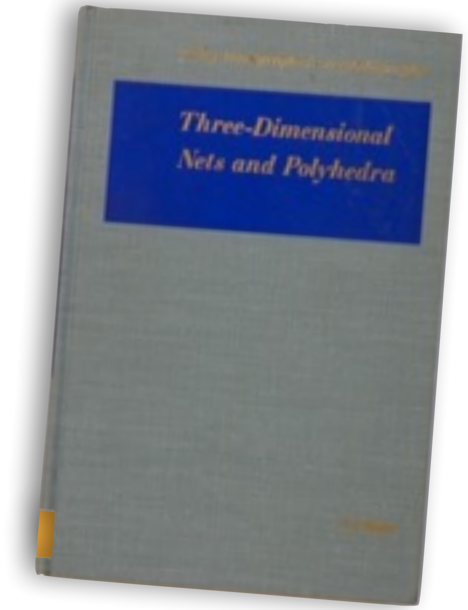

A.F.Wells, 1977

(9,3)

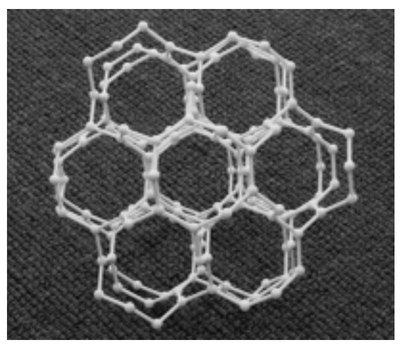
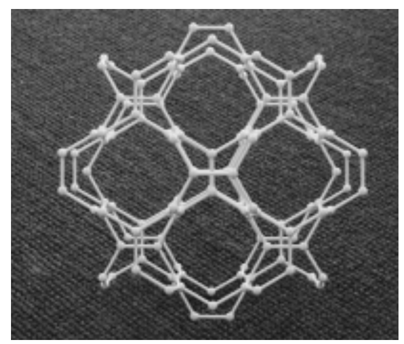

(8,3)

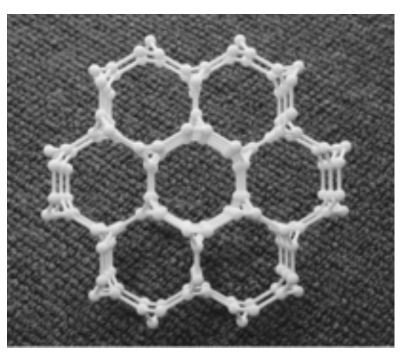
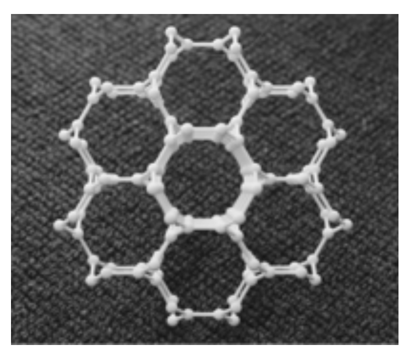
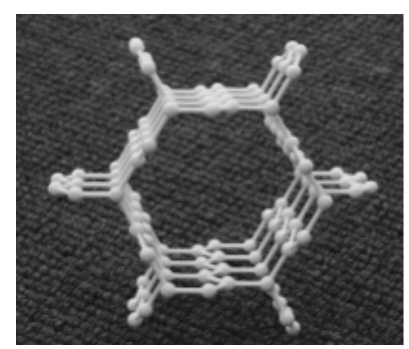
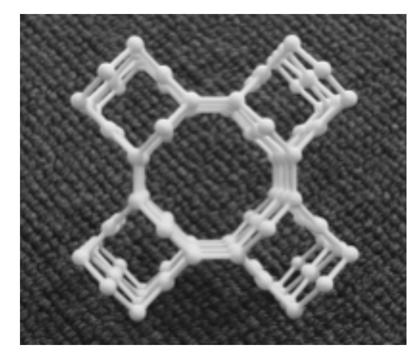

Tricoordinated lattices in 3D

- equal bond length
- 120° bond angles

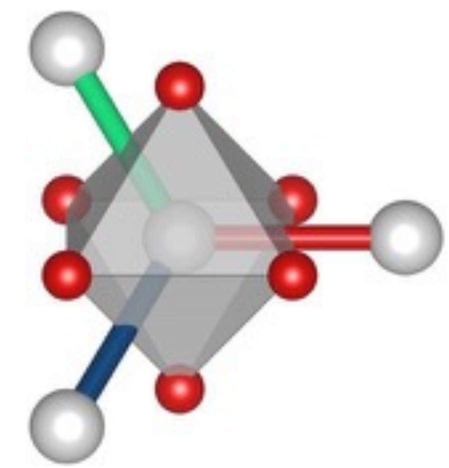

(10,3)

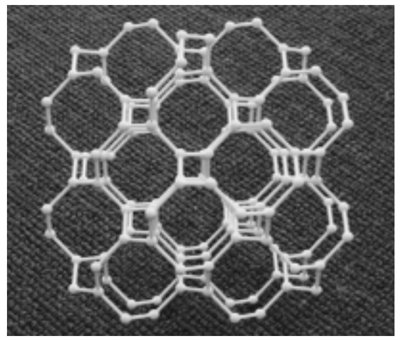

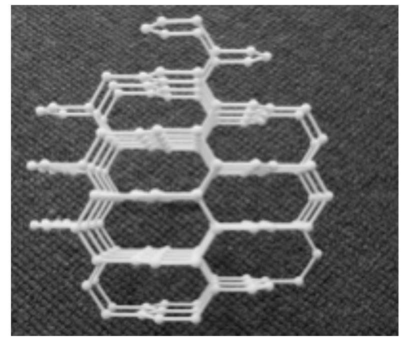

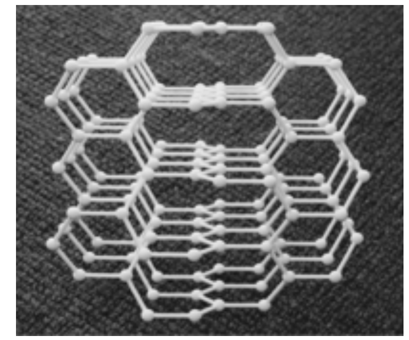

(9,3)

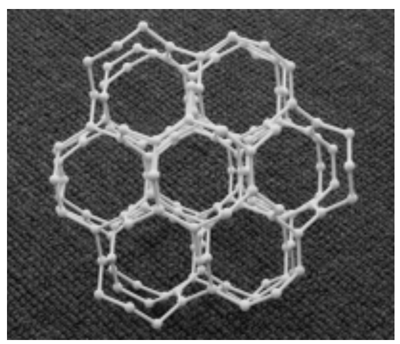

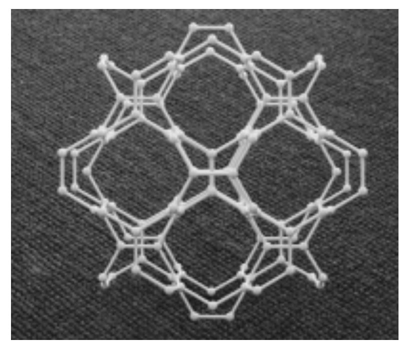

(8,3)

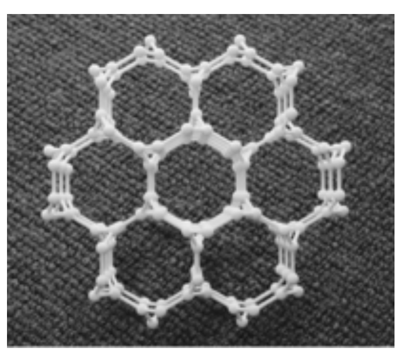

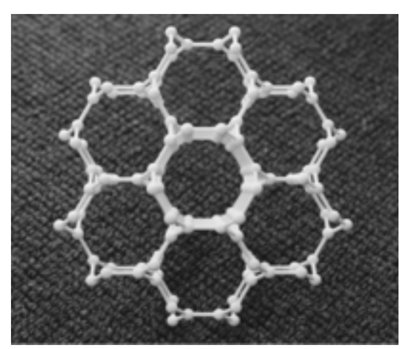

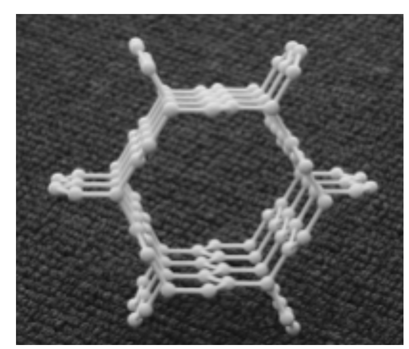

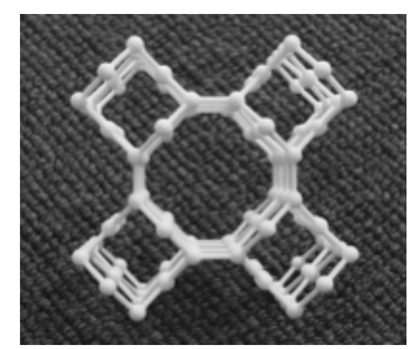

Tricoordinated lattices in 3D

Schäfli symbol	alternative names	atoms per unit cell	Inversion	Lieb theorem	space group
(10,3)a	hyperoctagon K4 lattice	4	✗	✗	$I4_132$ (214)
(10,3)b	hyperhoneycomb	4	✓	✗	Fddd (70)
(10,3)c	-	6	✗	✗	$P3_12$ (151)
(9,3)a	-	12	✓	✗	R-3m (166)
(9,3)b	-	24	✓	✗	P42 / nmc (137)
(8,3)a	-	6	✗	✗	$P6_222$ (180)
(8,3)b	-	6	✓	✓	R-3m (166)
(8,3)c	-	8	✓	✗	$P6_3$ / mmc (194)
(8,3)n	-	16	✓	✗	I4 / mmm (139)
(6.3)	honeycomb	2	✓	✓	

3D Kitaev models

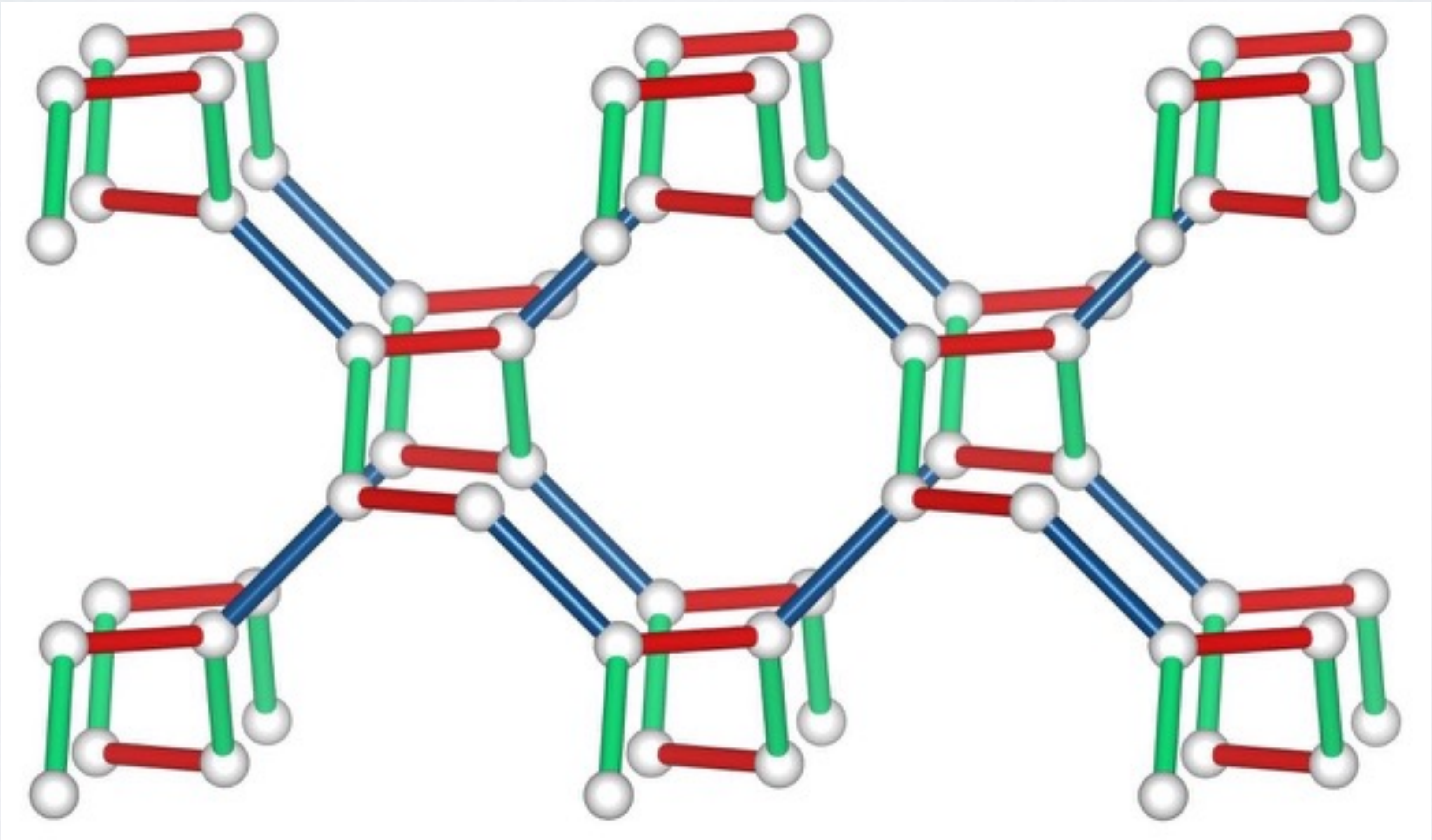

Spin fractionalization and Majorana fermions

A. Kitaev, Annals of Physics **321**, 2 (2006)

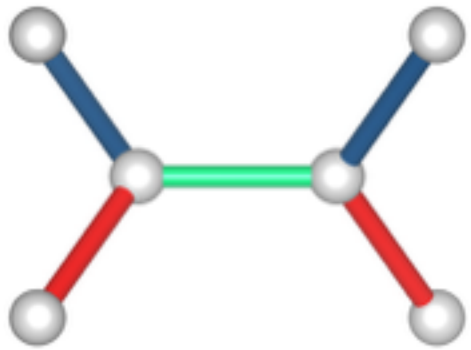

$$H = -\sum_{\gamma-\mathrm{bond}} J_\gamma \sigma_j^\gamma \sigma_k^\gamma$$

Spin fractionalization and Majorana fermions

A. Kitaev, Annals of Physics **321**, 2 (2006)

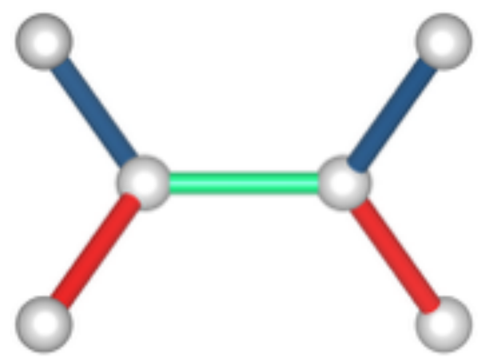

splitting spins

$$\sigma^\alpha = i a^\alpha c$$

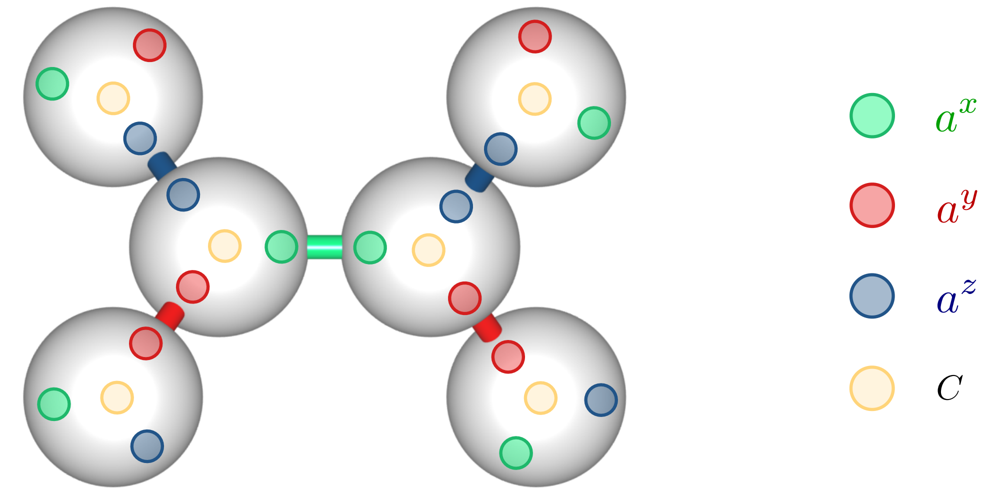

$$H = -\sum_{\gamma-\mathrm{bond}} J_\gamma \sigma_j^\gamma \sigma_k^\gamma$$

- represent spins by four **Majorana fermions**

Spin fractionalization and Majorana fermions

A. Kitaev, Annals of Physics **321**, 2 (2006)

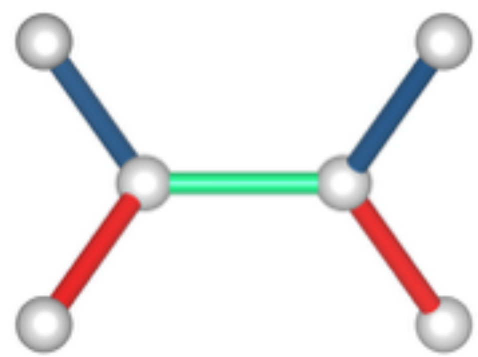

splitting spins

$$\sigma^\alpha = i a^\alpha c$$

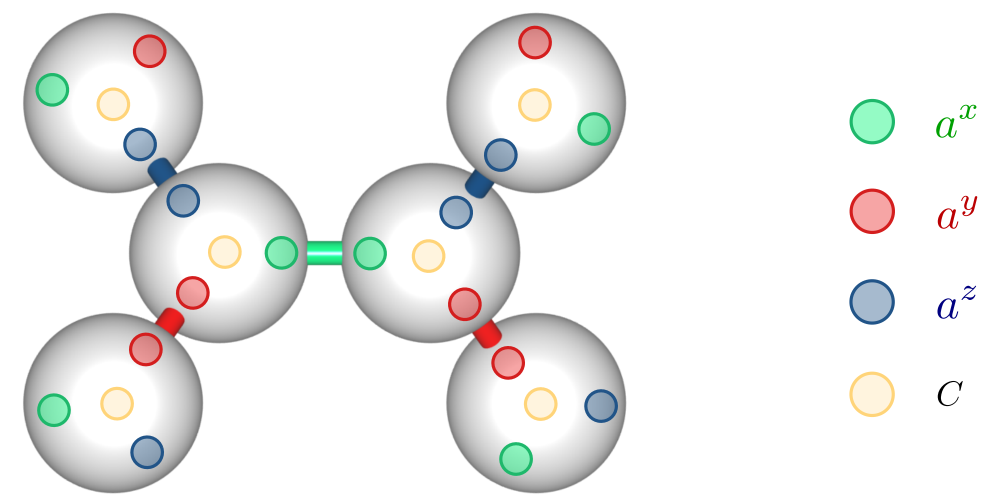

$$H = -\sum_{\gamma-\text{bond}} J_\gamma \sigma_j^\gamma \sigma_k^\gamma$$

joining Majoranas

$$\hat{u}_{jk} = i a_j^\alpha a_k^\alpha$$

- represent spins by four **Majorana fermions**
- emergent $\mathbf{Z_2}$ **gauge field** on bonds

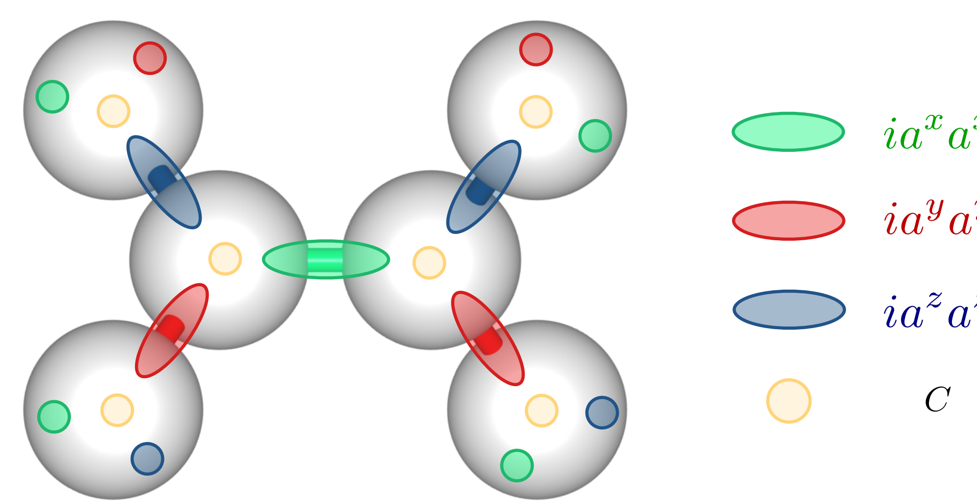

Spin fractionalization and Majorana fermions

A. Kitaev, Annals of Physics **321**, 2 (2006)

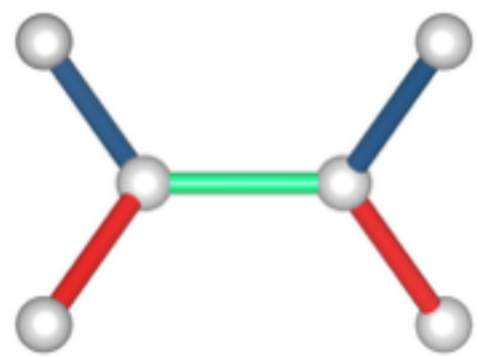

splitting spins

$$\sigma^\alpha = i a^\alpha c$$

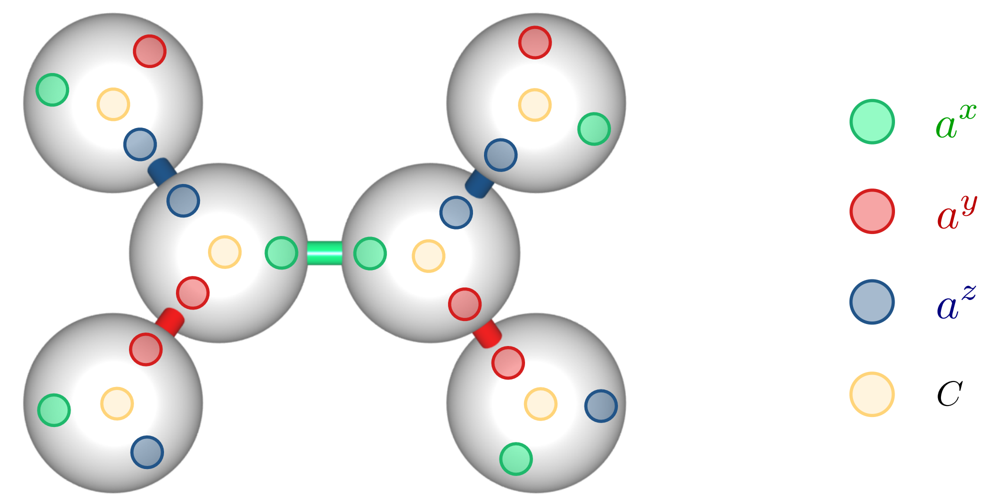

$$H = - \sum_{\gamma-\text{bond}} J_\gamma \sigma_j^\gamma \sigma_k^\gamma$$

joining Majoranas

$$\hat{u}_{jk} = i a_j^\alpha a_k^\alpha$$

- represent spins by four **Majorana fermions**
- emergent **Z_2 gauge field** on bonds
- Hilbert space split into two separate sectors: $2^N = 2^{N/2} \times 2^{N/2}$

Majorana fermions c_j "**spinons**"

flux loops "**visons**" (static and gapped)

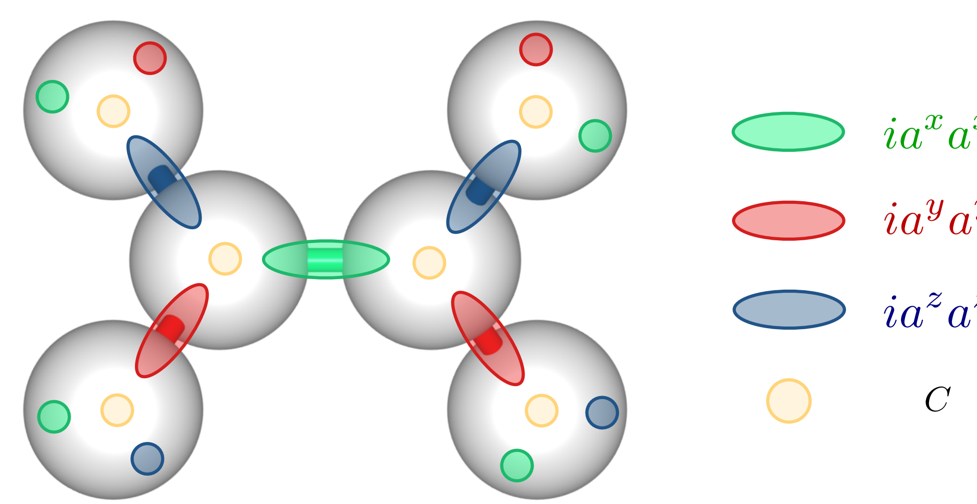

Spin fractionalization and Majorana fermions

A. Kitaev, Annals of Physics **321**, 2 (2006)

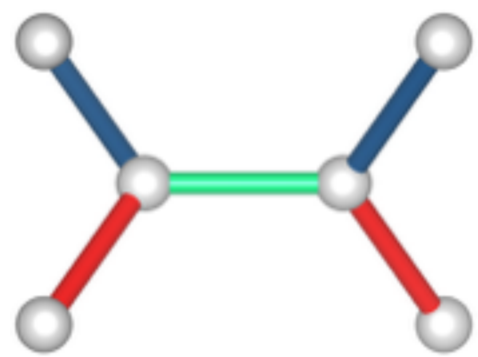

splitting spins

$$\sigma^\alpha = i a^\alpha c$$

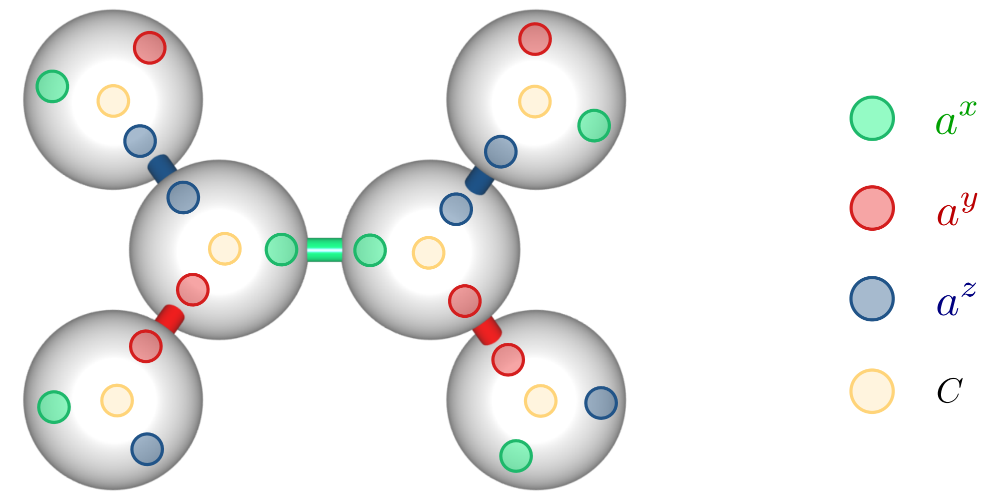

$$H = i \sum_{\gamma-\text{bond}} J_\gamma c_j c_k$$

joining Majoranas

$$\hat{u}_{jk} = i a_j^\alpha a_k^\alpha$$

- represent spins by four **Majorana fermions**
- emergent **Z_2 gauge field** on bonds
- Hilbert space split into two separate sectors: $2^N = 2^{N/2} \times 2^{N/2}$

Majorana fermions c_j "**spinons**"

flux loops "**visons**" (static and gapped)

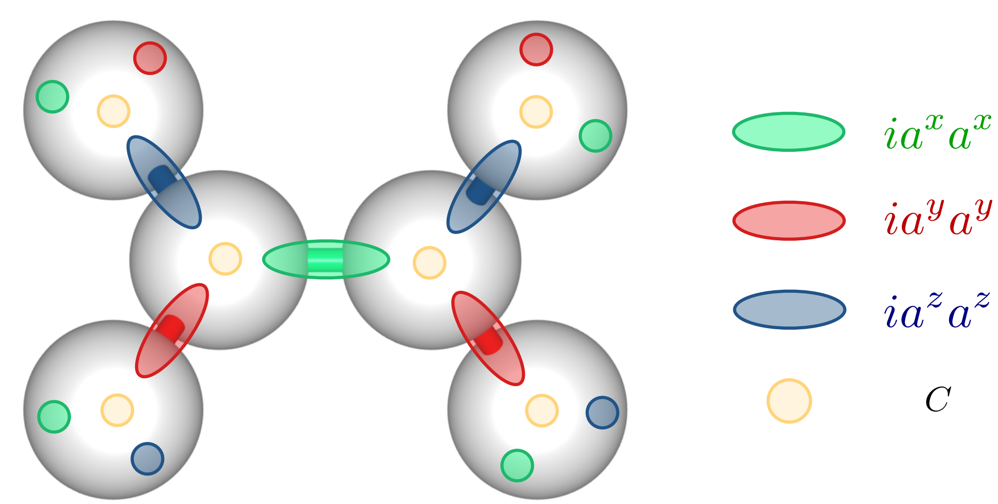

Kitaev spin liquids in 2D

Kitaev, Annals of Physics ’06

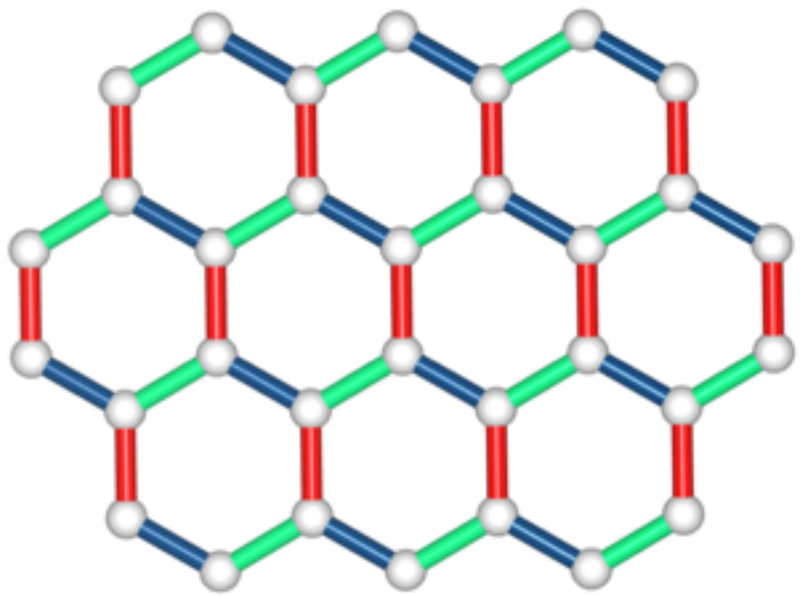

$$H = i \sum_{\gamma-\mathrm{bond}} J_\gamma c_j c_k$$

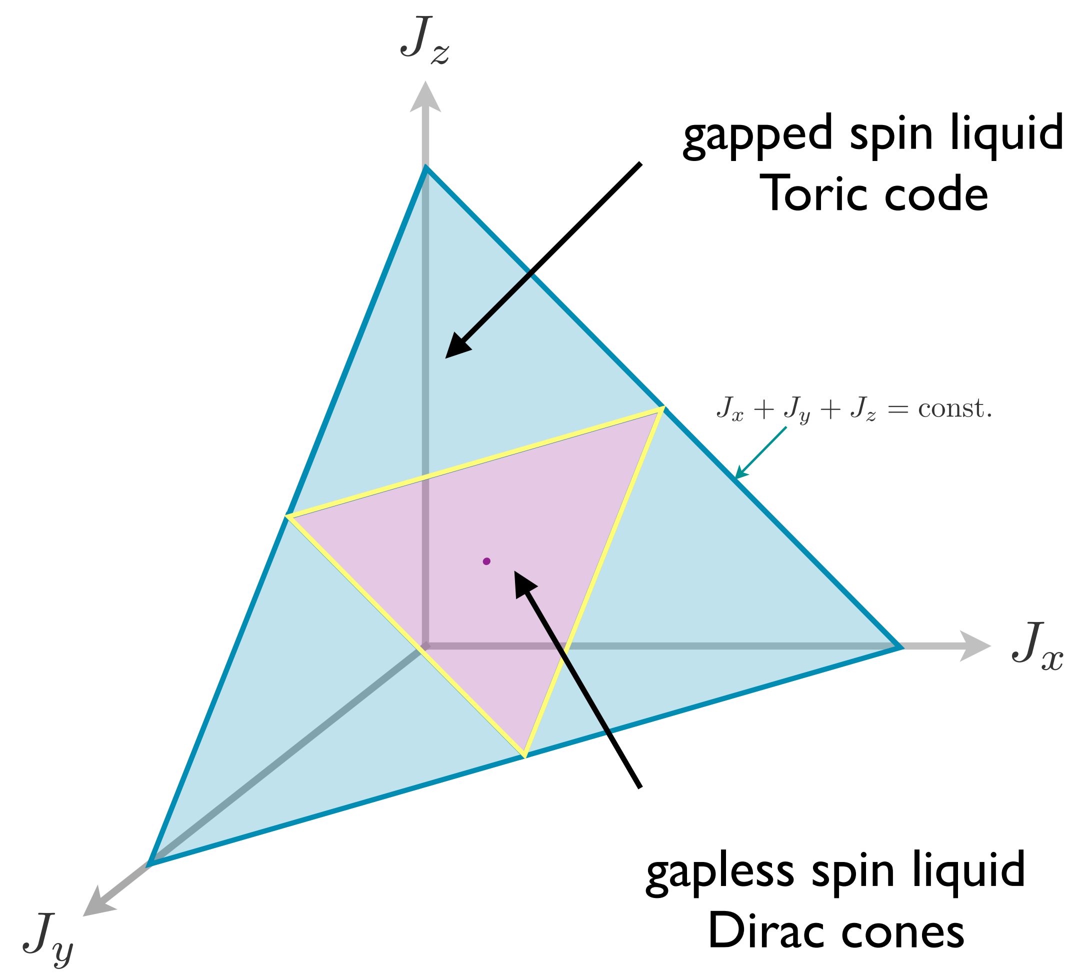

Kitaev spin liquids in 2D

Kitaev, Annals of Physics ’06

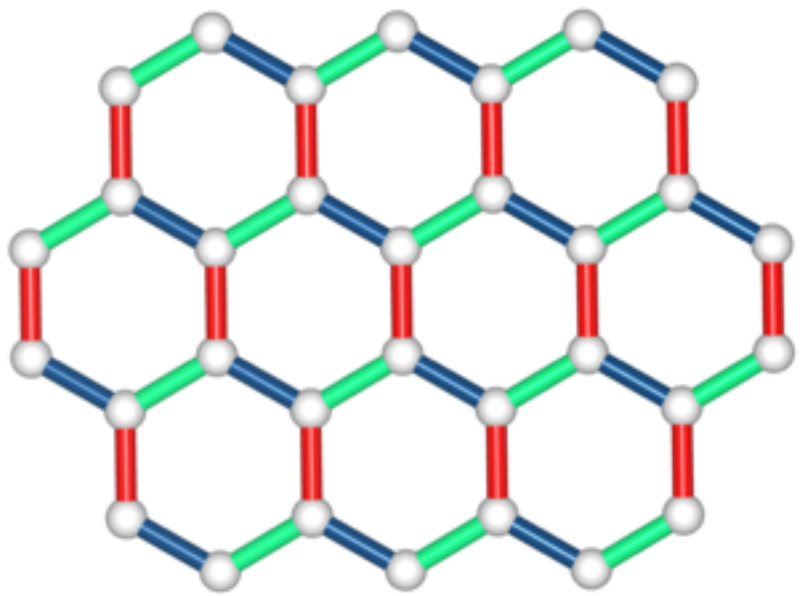

$$H = i \sum_{\gamma-\text{bond}}$$

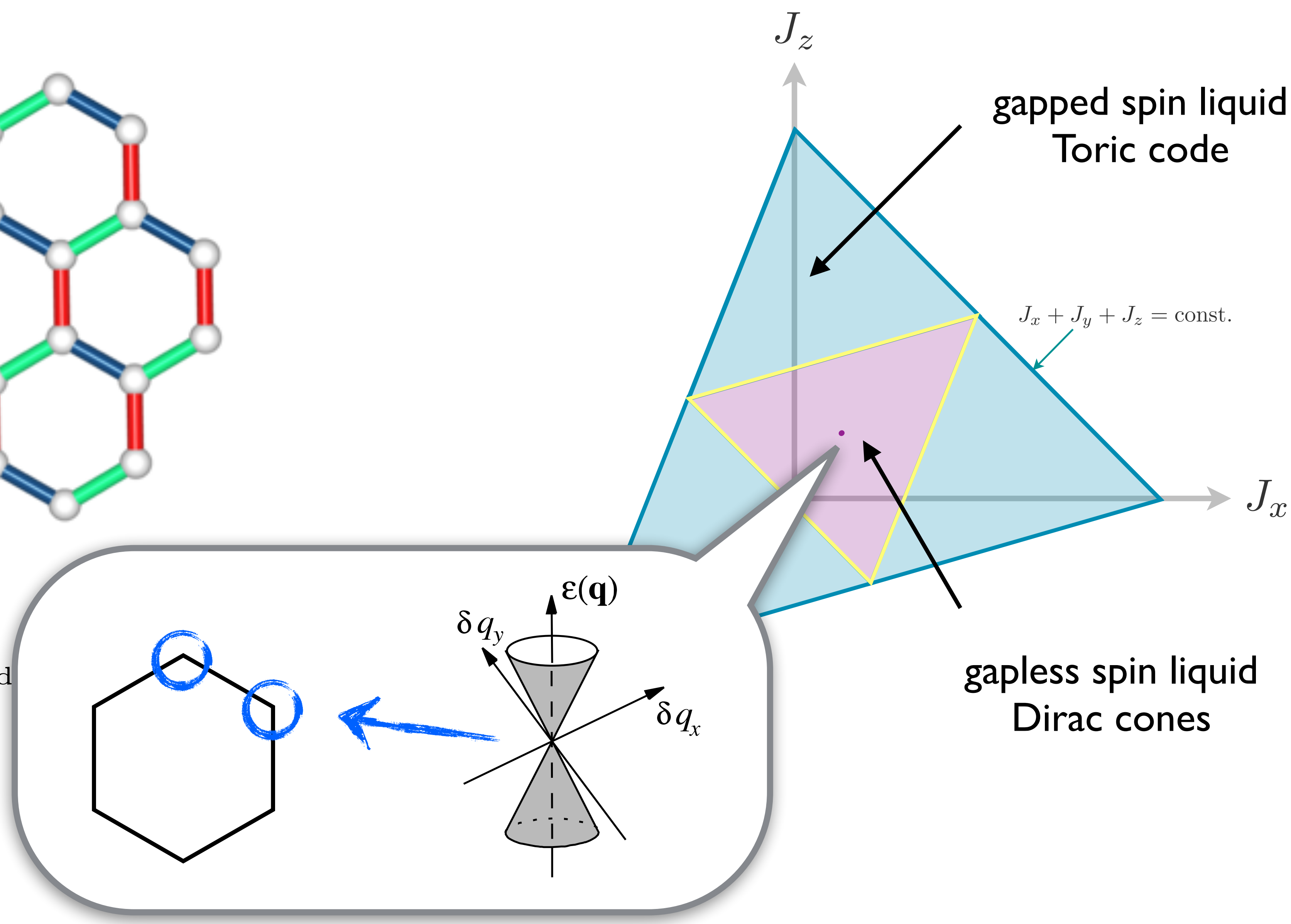

Kitaev models in 3D

Schäfli symbol	Majorana metal	TR breaking	Peierls instability
(10,3)a (hyperoctagon)	(topological) Fermi surface	(topological) Fermi surface	✓
(10,3)b (hyperhoneycomb)	Fermi line	Weyl nodes	✗
(10,3)c	Fermi line	topological Fermi surface	✗
(9,3)a	Weyl nodes	Weyl nodes	✗
(9,3)b	-	-	✗
(8,3)a	(topological) Fermi surface	(topological) Fermi surface	✓
(8,3)b	Weyl nodes	Weyl nodes	✓
(8,3)c	Fermi line	Weyl nodes	✗
(8,3)n	gapped	gapped	✗
(6,3)a (honeycomb)	Dirac points	gapped NA	✗

Kitaev models in 3D

Schäfli symbol	Majorana metal	TR breaking	Peierls instability
(10,3)a (hyperoctagon)	(topological) Fermi surface	(topological) Fermi surface	✓
(10,3)b (hyperhoneycomb)	Fermi line	Weyl nodes	✗
(10,3)c	Fermi line	topological Fermi surface	✗
(9,3)a	Weyl nodes	Weyl nodes	✗
(9,3)b	-	-	✗
(8,3)a	(topological) Fermi surface	(topological) Fermi surface	✓
(8,3)b	Weyl nodes	Weyl nodes	✓
(8,3)c	Fermi line	Weyl nodes	✗
(8,3)n	gapped	gapped	✗
(6,3)a (honeycomb)	Dirac points	gapped NA	✗

(10,3)a – Majorana Fermi surface

M.H., S. Trebst, PRB 89, 235102 (2014)

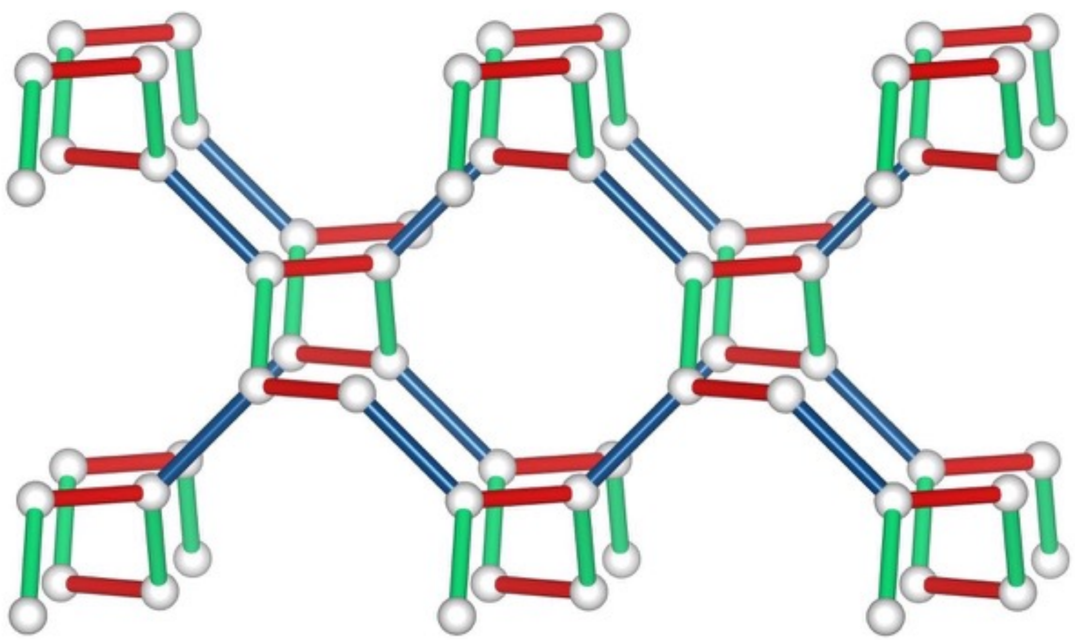

$$H = i \sum_{\gamma-\text{bond}} J_\gamma c_j c_k$$

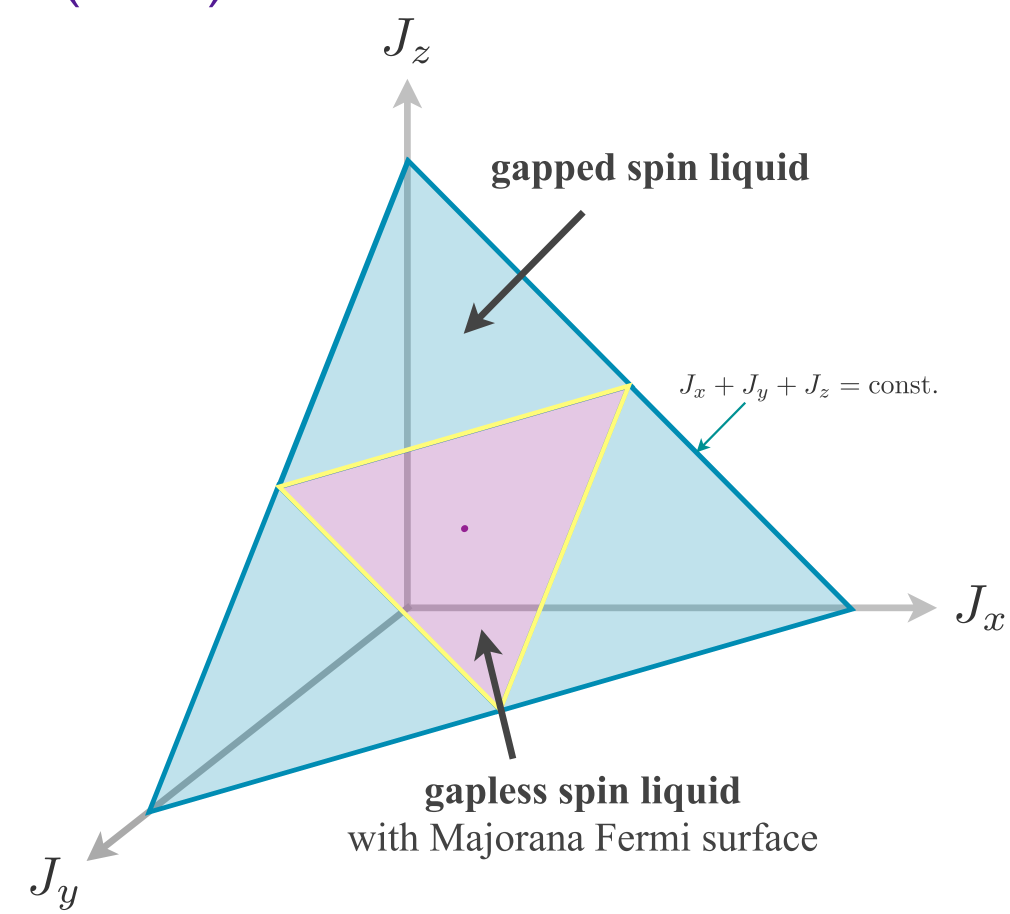

(10,3)a – Majorana Fermi surface

M.H., S. Trebst, PRB 89, 235102 (2014)

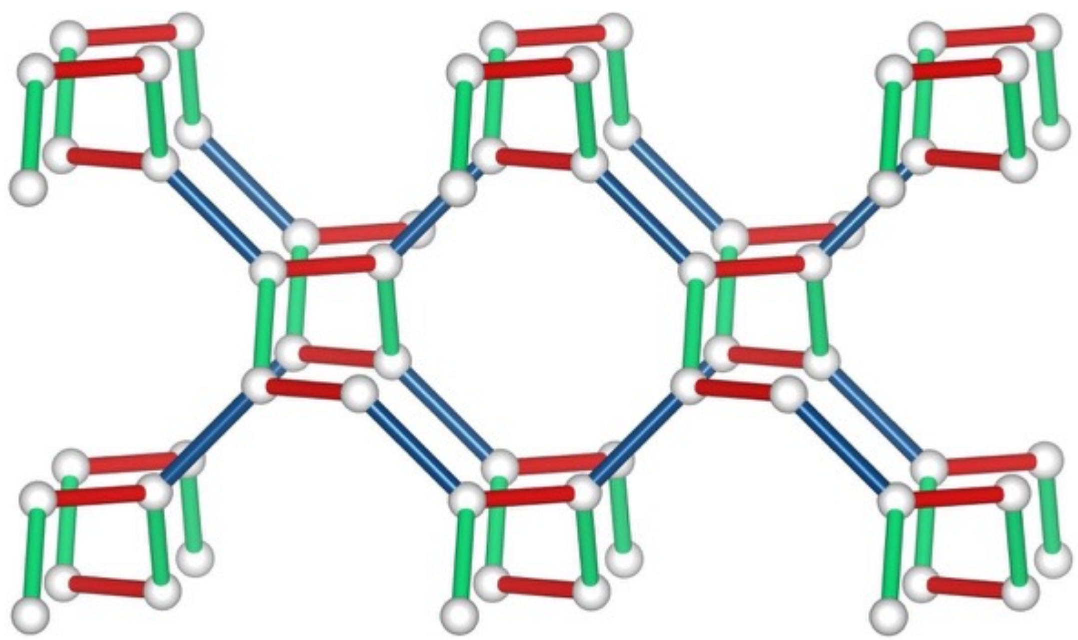

$$H = i \sum_{\gamma-\text{bond}} J_\gamma c_j c_k$$

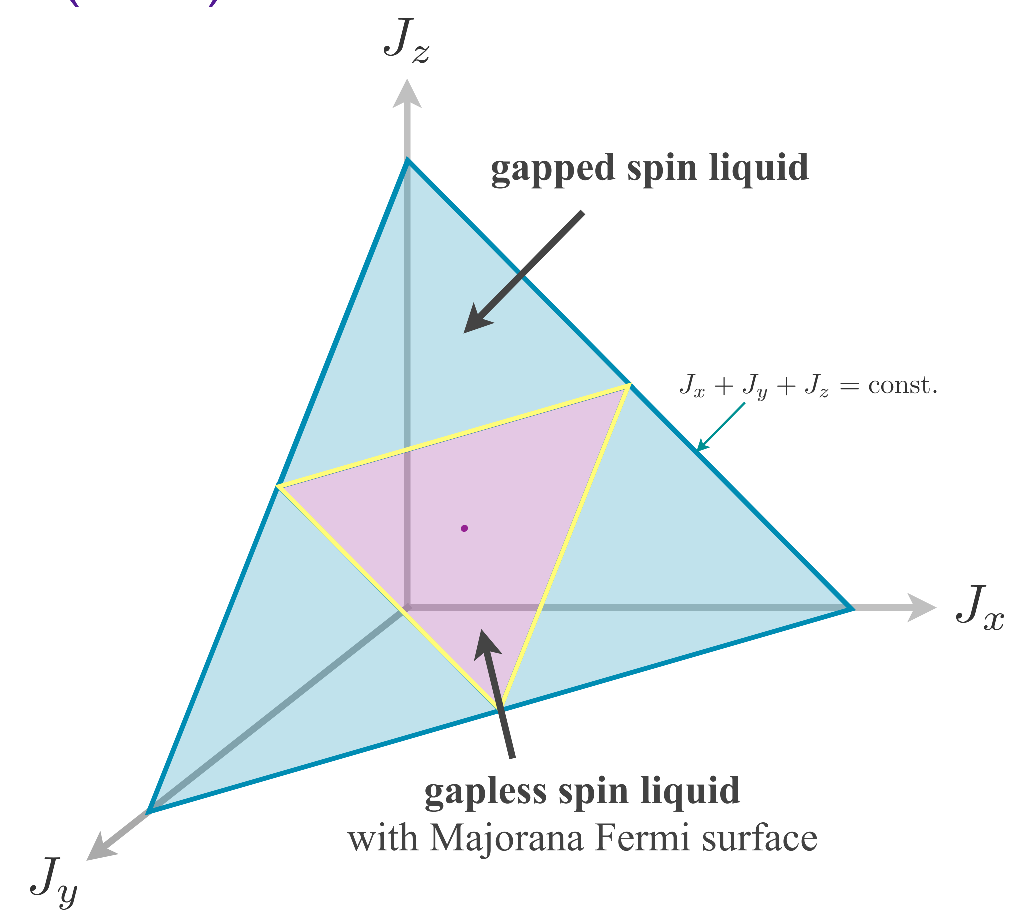

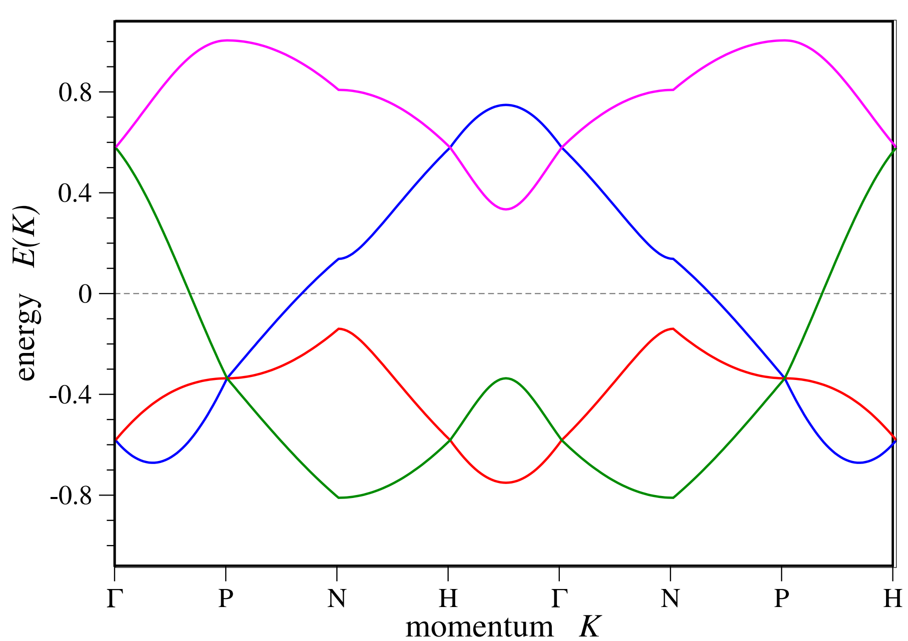

(10,3)a – Majorana Fermi surface

M.H., S. Trebst, PRB 89, 235102 (2014)

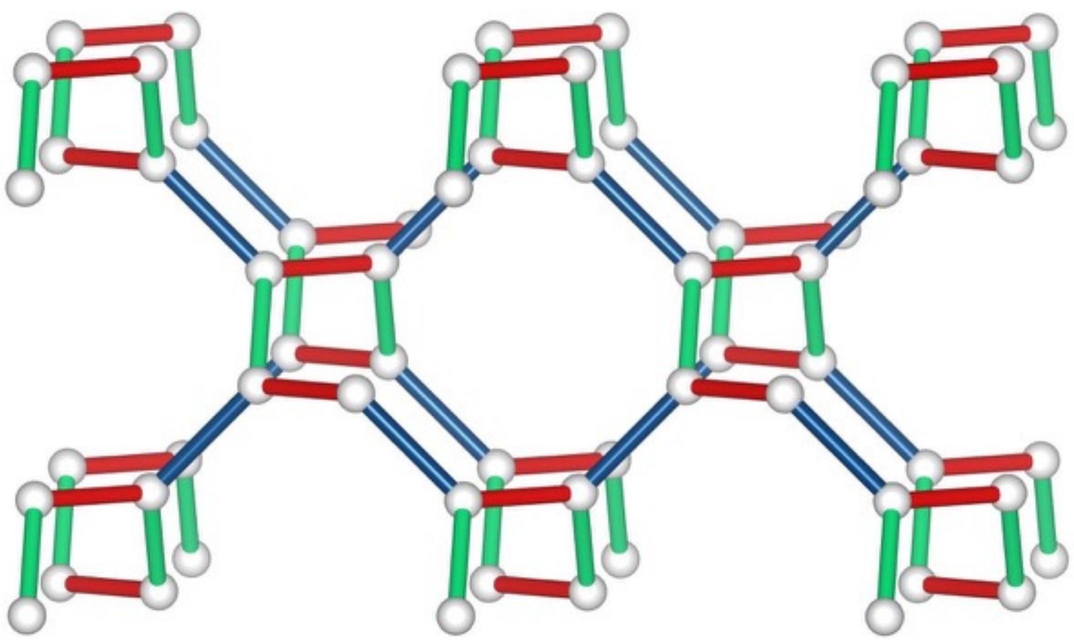

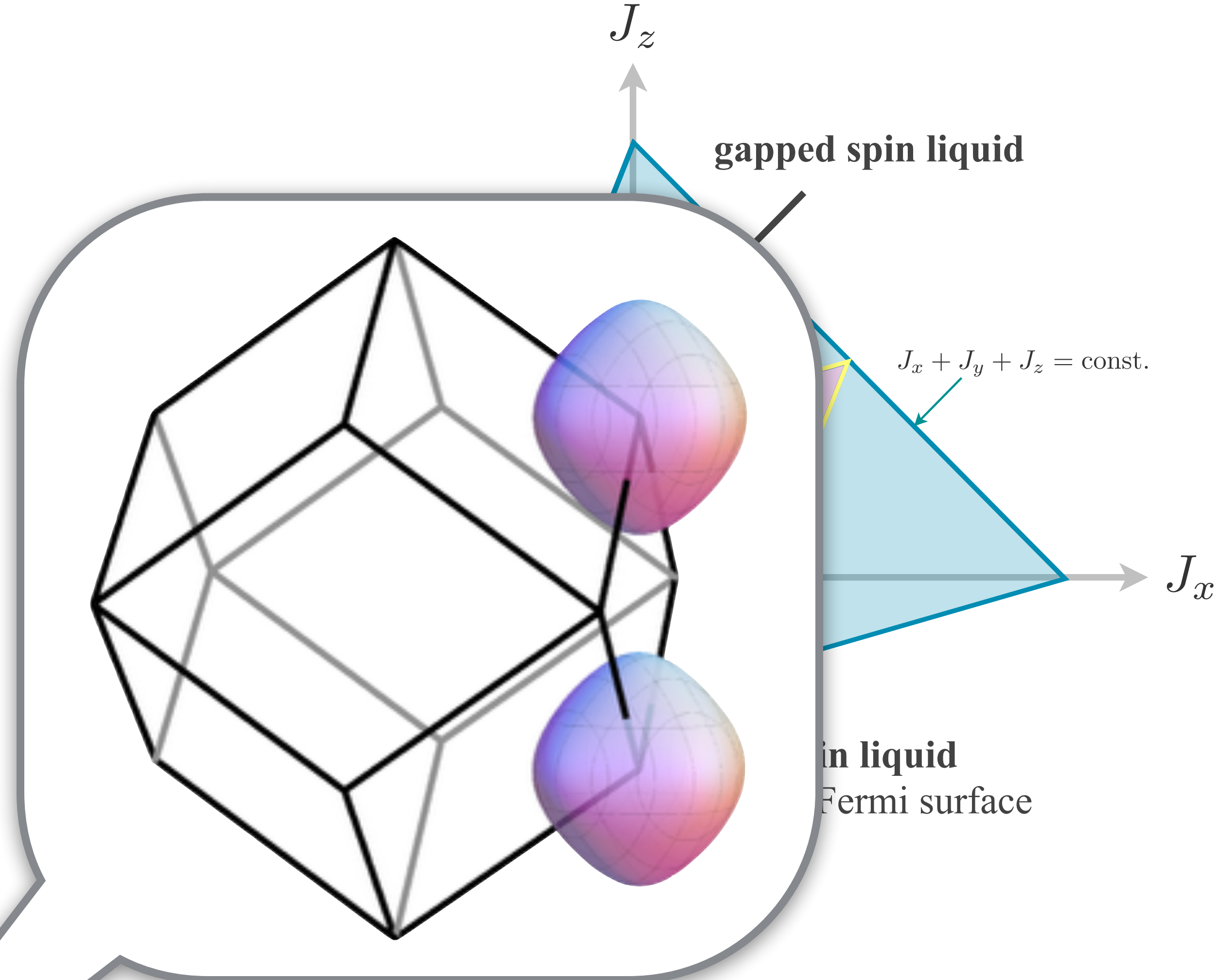

$$H = i \sum_{\gamma-\text{bond}} J_\gamma c_j c_k$$

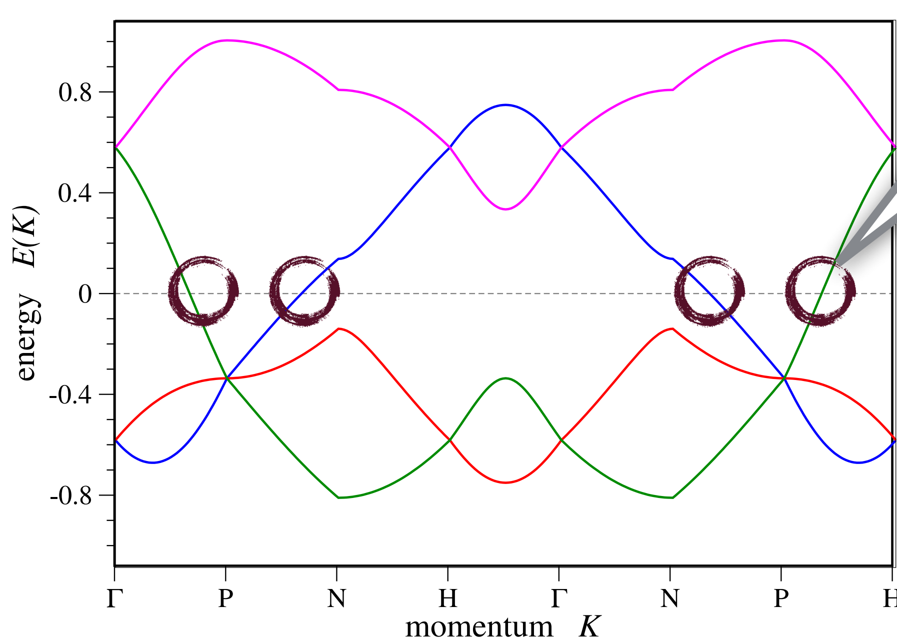

(10,3)a – Majorana Fermi surface

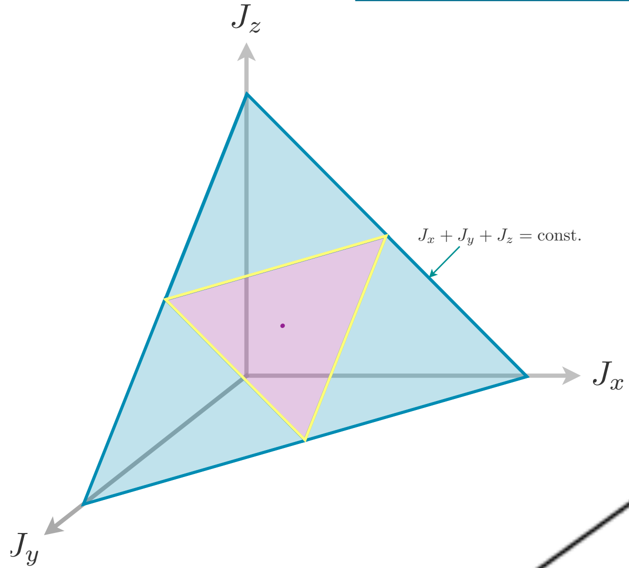

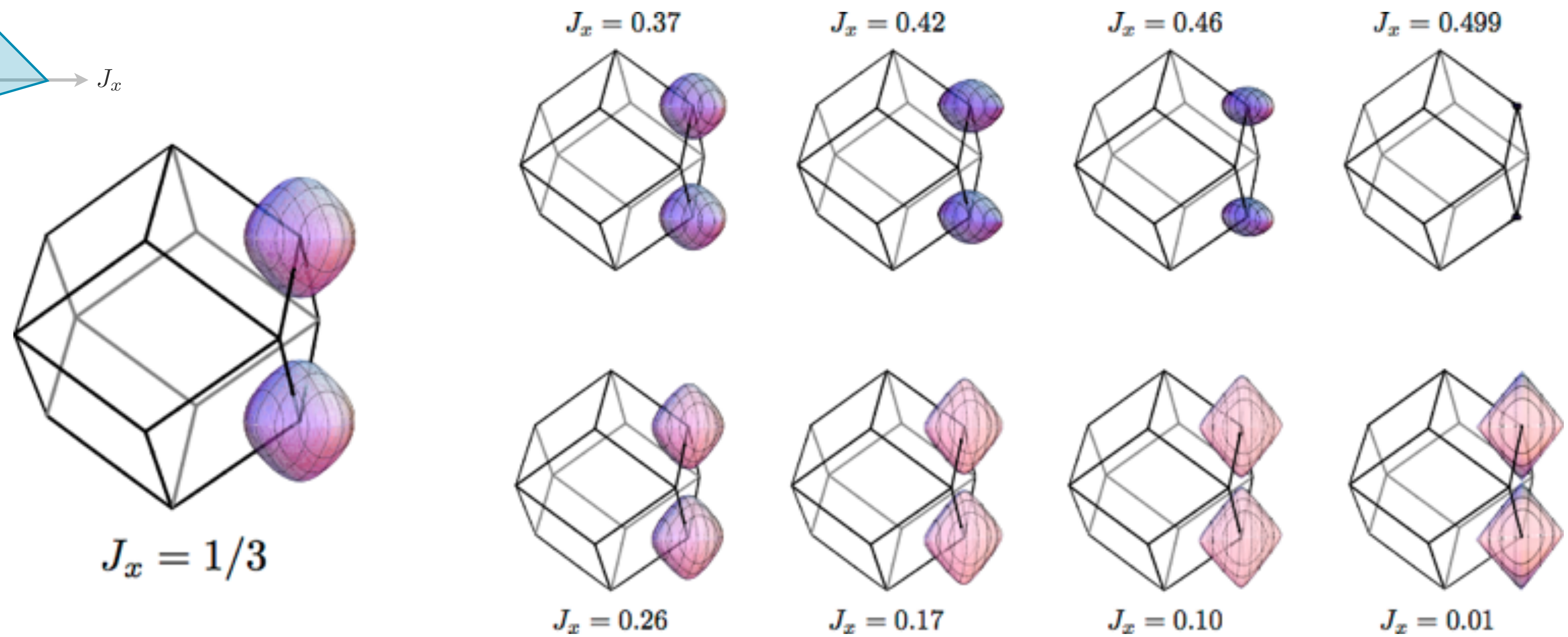

stable Majorana Fermi surface throughout the gapless region
Z_2 spin liquid with spinon Fermi surface

Spin-Peierls BCS instability

M.H., S. Trebst, A. Rosch, arXiv:1506.01379 (2015)

natural BCS-type instability for time-reversal invariant systems

Majorana fermions c_k
→ perfect nesting

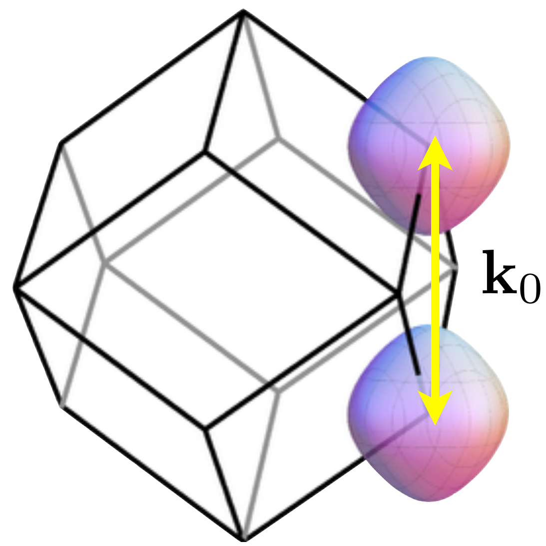

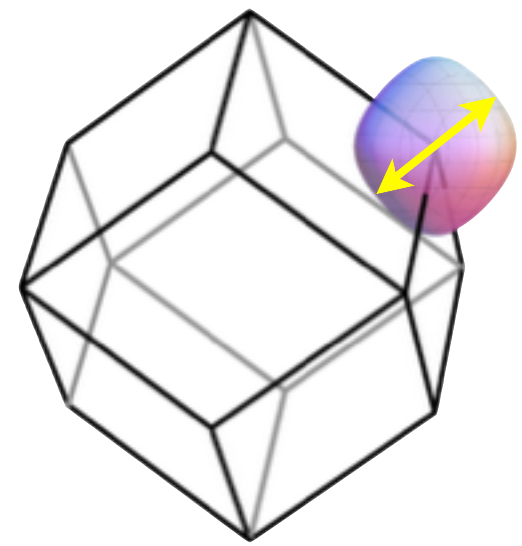

complex fermion f_k
→ BCS pairing

Spin-Peierls BCS instability

M.H., S. Trebst, A. Rosch, arXiv:1506.01379 (2015)

natural BCS-type instability for time-reversal invariant systems

Majorana fermions c_k
→ perfect nesting

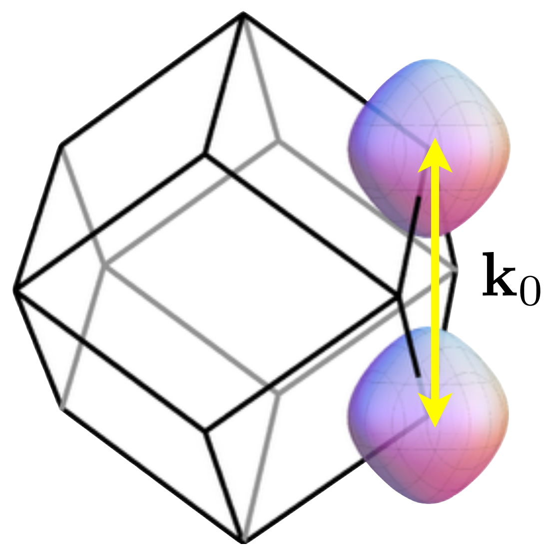

complex fermion f_k
→ BCS pairing

Fermi surface centered around $\mathbf{k}_0/2$

order parameter has finite momentum $\mathbf{k}_0$: $\Delta \sim \langle f^\dagger_{\mathbf{k}_0+\mathbf{q}} f^\dagger_{\mathbf{k}_0-\mathbf{q}} \rangle$

spontanous breaking of translational symmetry

↪ spin-Peierls transition

additional breaking of rotation symmetry possible

order parameter distribution

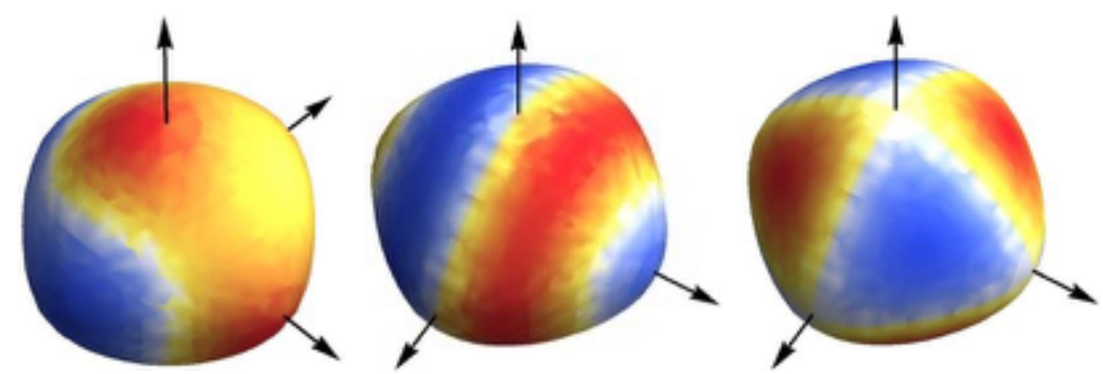

Spin-Peierls BCS instability

M.H., S. Trebst, A. Rosch, arXiv:1506.01379 (2015)

Perfect nesting condition is destroyed by TR breaking

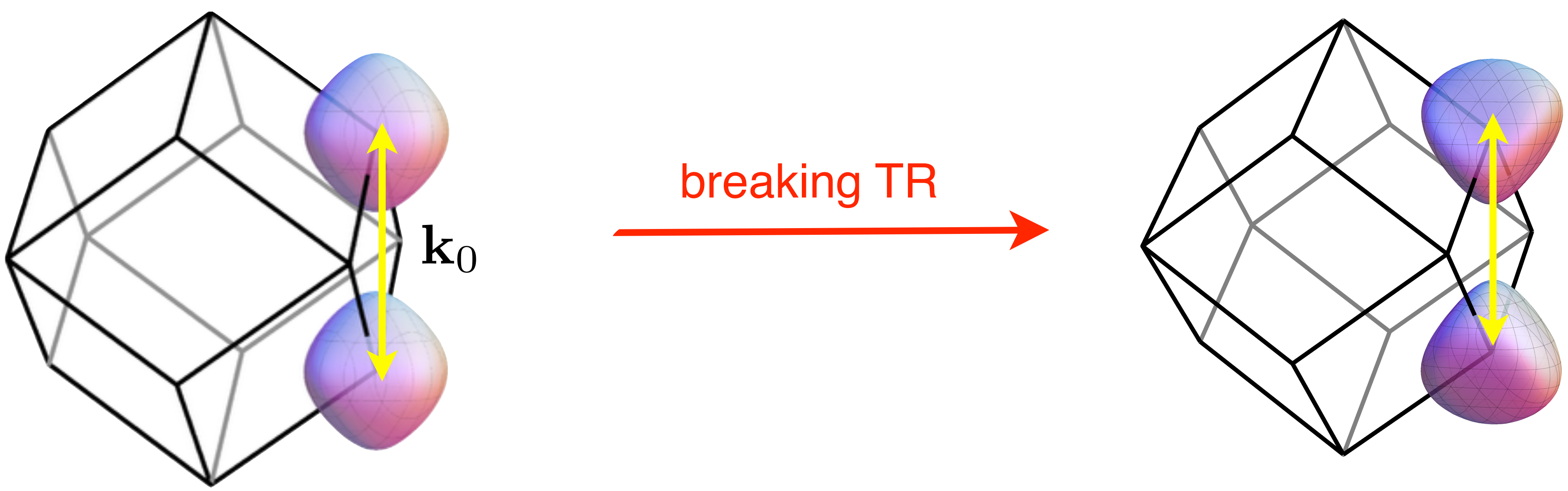

BCS instability cut-off at low temperatures

Time-reversal breaking stabilizes Majorana Fermi surface

(10,3)b – Fermi line

Mandal, Surendran, PRB 79, 024426 (2009)
Lee etal., PRB 89, 014424 (2014)
Kimchi, Analytis, Vishwanath, PRB 90, 205126 (2014)
Nasu, Udagawa, Motome, PRL 113, 197205 (2014)

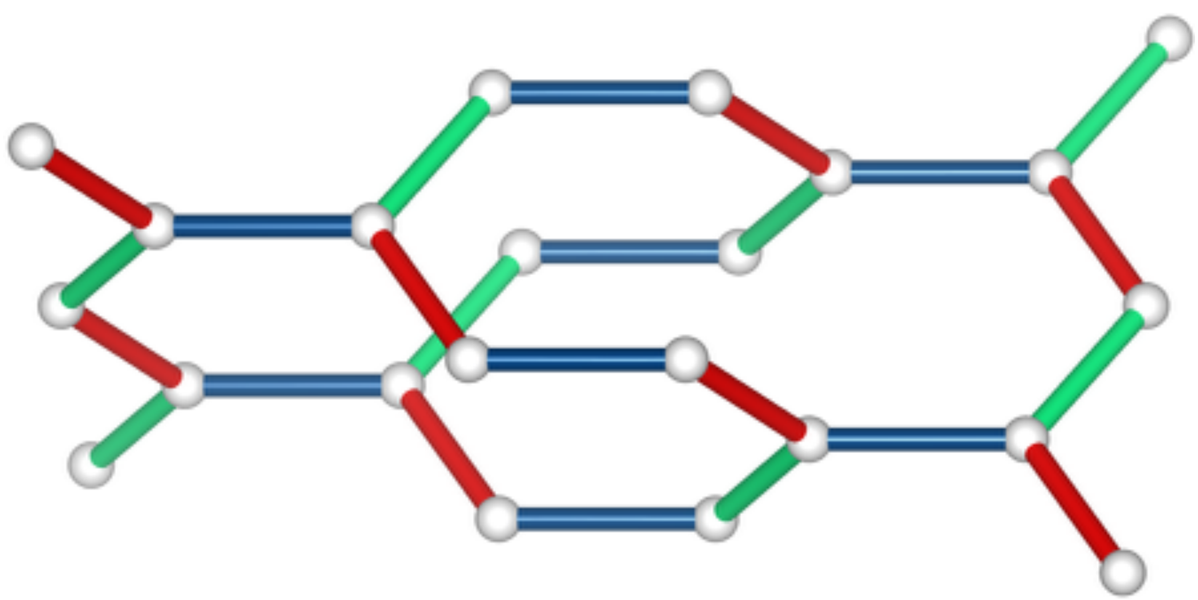

$$H = i \sum_{\gamma-\text{bond}} J_\gamma c_j c_k$$

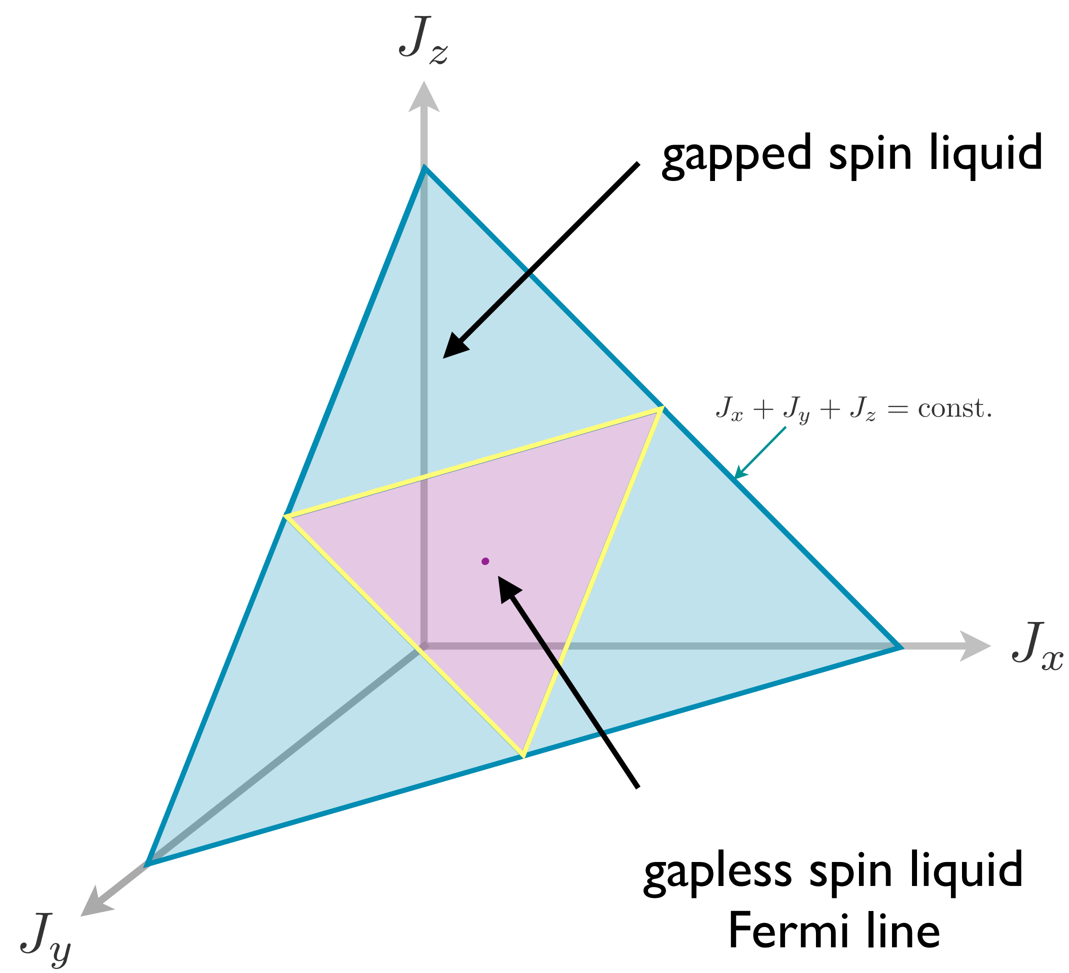

(10,3)b – Fermi line

Mandal, Surendran, PRB 79, 024426 (2009)
Lee etal., PRB 89, 014424 (2014)
Kimchi, Analytis, Vishwanath, PRB 90, 205126 (2014)
Nasu, Udagawa, Motome, PRL 113, 197205 (2014)

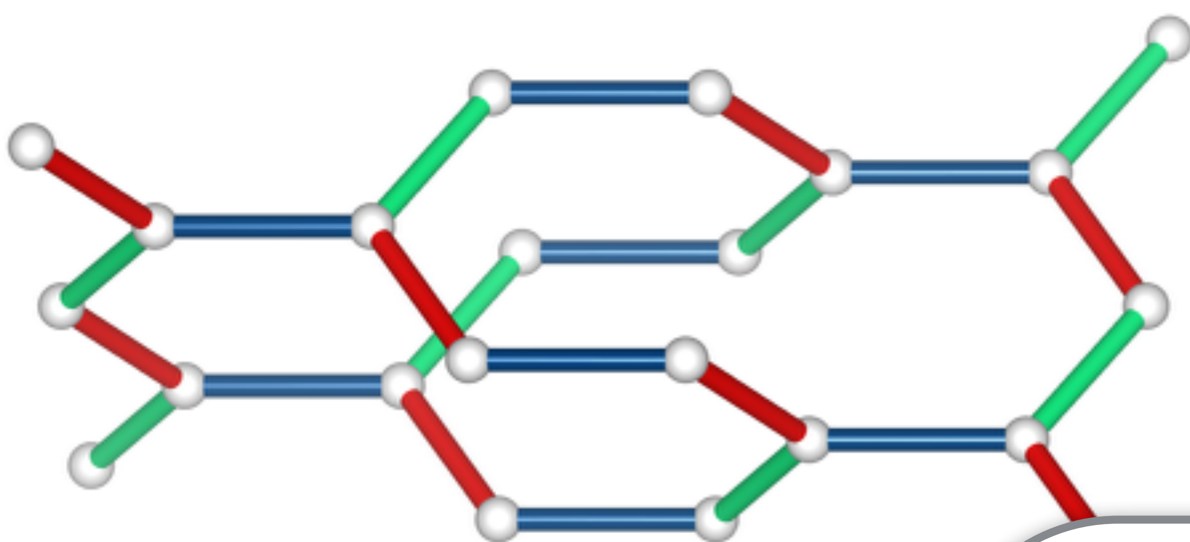

$$H = i \sum_{\gamma-\mathrm{bond}} J_\gamma c_j c_k$$

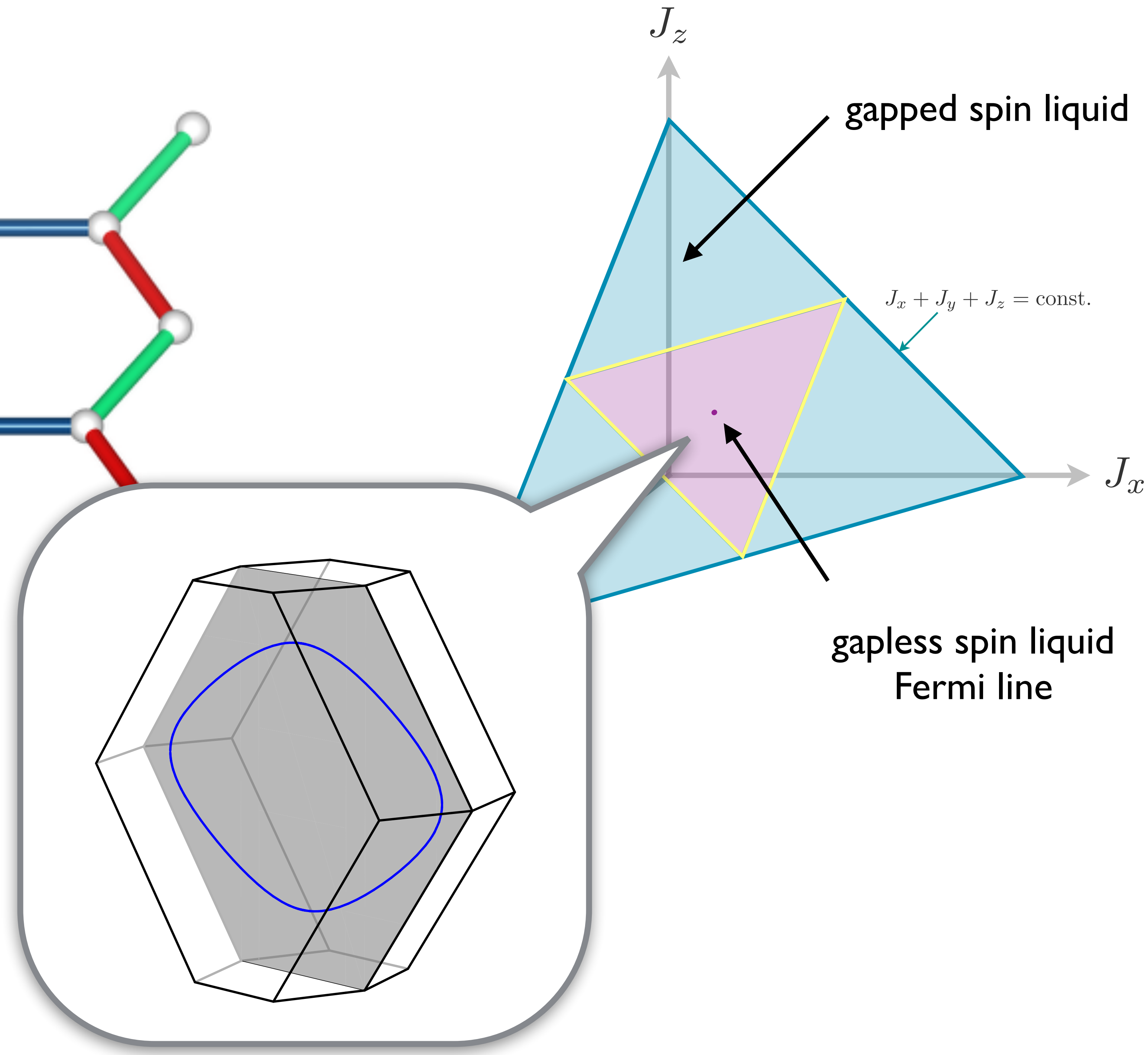

Symmetries in Majorana systems

M.H., S. Trebst, PRB 89, 235102 (2014)

Particle-hole symmetry	$\epsilon(\mathbf{k}) = -\epsilon(-\mathbf{k})$

$\mathbf{k}_0$ is the reciprocal lattice vector of the sublattice

Symmetries in Majorana systems

M.H., S. Trebst, PRB 89, 235102 (2014)

Particle-hole symmetry	$\epsilon(\mathbf{k}) = -\epsilon(-\mathbf{k})$
Sublattice symmetry	$\epsilon(\mathbf{k}) = -\epsilon(\mathbf{k} - \mathbf{k}_0)$

$\mathbf{k}_0$ is the reciprocal lattice vector of the sublattice

hyperhoneycomb

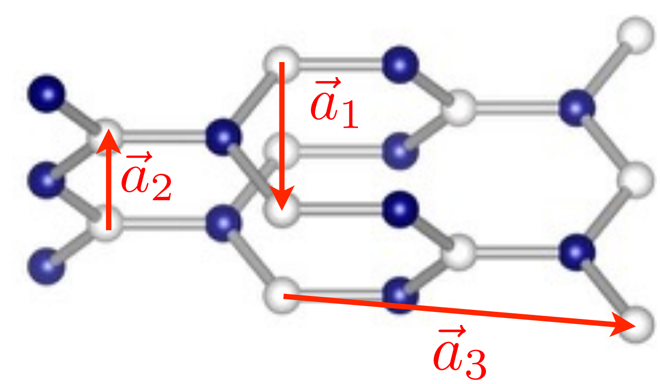

$\mathbf{k}_0 = 0$

hyperoctagon

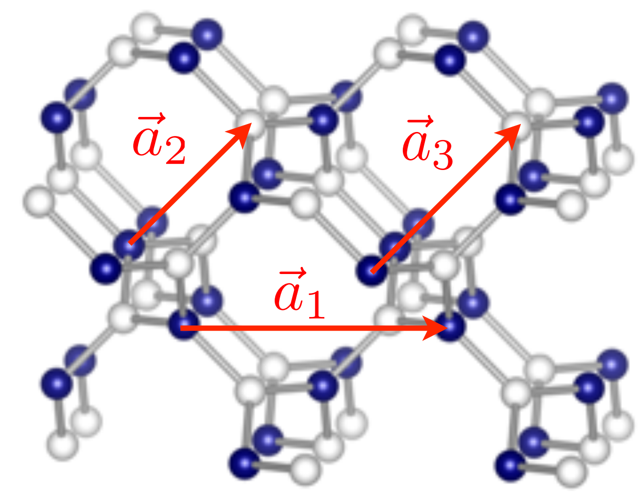

$\mathbf{k}_0 = (\mathbf{q}_2 + \mathbf{q}_3)/2$

Symmetries in Majorana systems

M.H., S. Trebst, PRB 89, 235102 (2014)

Particle-hole symmetry	$\epsilon(\mathbf{k}) = -\epsilon(-\mathbf{k})$
Sublattice symmetry	$\epsilon(\mathbf{k}) = -\epsilon(\mathbf{k} - \mathbf{k}_0)$
Time-reversal symmetry	$\epsilon(\mathbf{k}) = \epsilon(-\mathbf{k} + \mathbf{k}_0)$

$\mathbf{k}_0$ is the reciprocal lattice vector of the sublattice

hyperhoneycomb

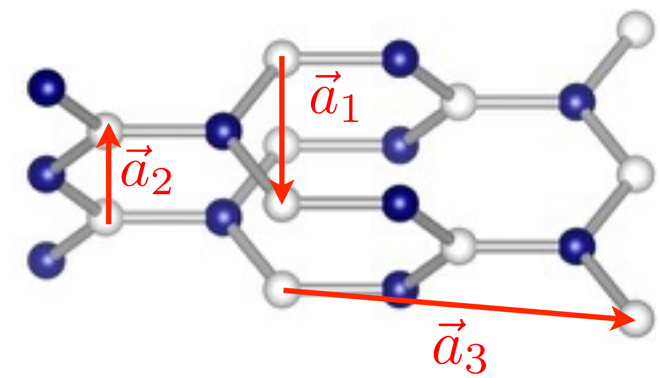

$\mathbf{k}_0 = 0$

hyperoctagon

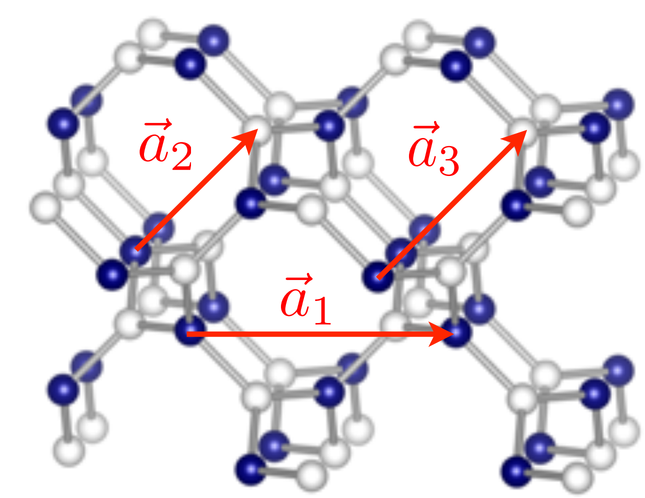

$\mathbf{k}_0 = (\mathbf{q}_2 + \mathbf{q}_3)/2$

Symmetries in Majorana systems

M.H., S. Trebst, PRB 89, 235102 (2014)

Particle-hole symmetry	$\epsilon(\mathbf{k}) = -\epsilon(-\mathbf{k})$
Sublattice symmetry	$\epsilon(\mathbf{k}) = -\epsilon(\mathbf{k} - \mathbf{k}_0)$
Time-reversal symmetry	$\epsilon(\mathbf{k}) = \epsilon(-\mathbf{k} + \mathbf{k}_0)$

hyperhoneycomb

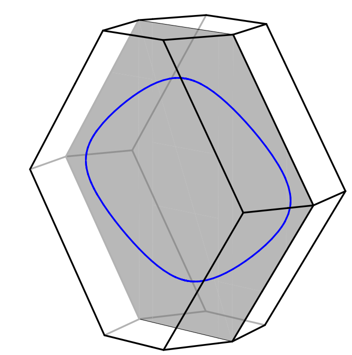

$\mathbf{k}_0 = 0$

hyperoctagon

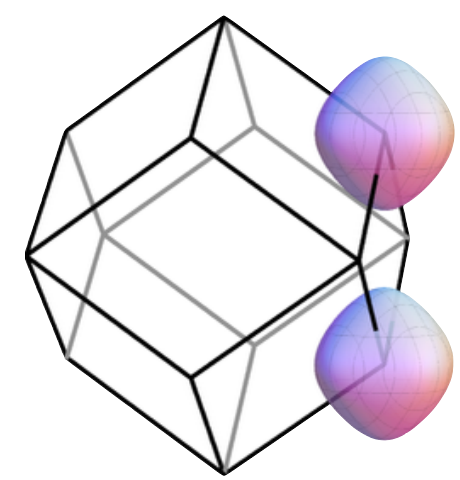

$\mathbf{k}_0 = (\mathbf{q}_2 + \mathbf{q}_3)/2$

$\mathbf{k}_0$ is the reciprocal lattice vector of the sublattice

$\mathbf{k}_0 = 0$: particle-hole symmetry at each **k**

- **separated points** (2D)
- **lines** (3D)

$\mathbf{k}_0 \neq 0$: generic band Hamiltonian

- **lines** (2D)
- **surfaces** (3D)

Kitaev models in 3D

Schäfli symbol	Majorana metal	TR breaking	Peierls instability
(10,3)a (hyperoctagon)	(topological) Fermi surface	(topological) Fermi surface	✓
(10,3)b (hyperhoneycomb)	Fermi line	Weyl nodes	✗
(10,3)c	Fermi line	topological Fermi surface	✗
(9,3)a	Weyl nodes	Weyl nodes	✗
(9,3)b	-	-	✗
(8,3)a	(topological) Fermi surface	(topological) Fermi surface	✓
(8,3)b	Weyl nodes	Weyl nodes	✓
(8,3)c	Fermi line	Weyl nodes	✗
(8,3)n	gapped	gapped	✗
(6,3)a (honeycomb)	Dirac points	gapped NA	✗

Weyl physics

Touching of two bands in 3D is generically **linear**

$$\hat{H} = \vec{v}_0 \cdot \vec{q}\,\mathbb{1} + \sum_{j=1}^{3} \vec{v}_j \cdot \vec{q}\,\sigma_j$$ **Weyl nodes**

Weyl nodes are **sources/sinks of Berry flux**
with charge/chirality $\mathrm{sign}[\vec{v}_1 \cdot (\vec{v}_2 \times \vec{v}_3)]$

Weyl physics

Touching of two bands in 3D is generically **linear**

$$\hat{H} = \vec{v}_0 \cdot \vec{q}\,\mathbb{1} + \sum_{j=1}^{3} \vec{v}_j \cdot \vec{q}\,\sigma_j$$ **Weyl nodes**

Weyl nodes are **sources/sinks of Berry flux** with charge/chirality $\mathrm{sign}[\vec{v}_1 \cdot (\vec{v}_2 \times \vec{v}_3)]$

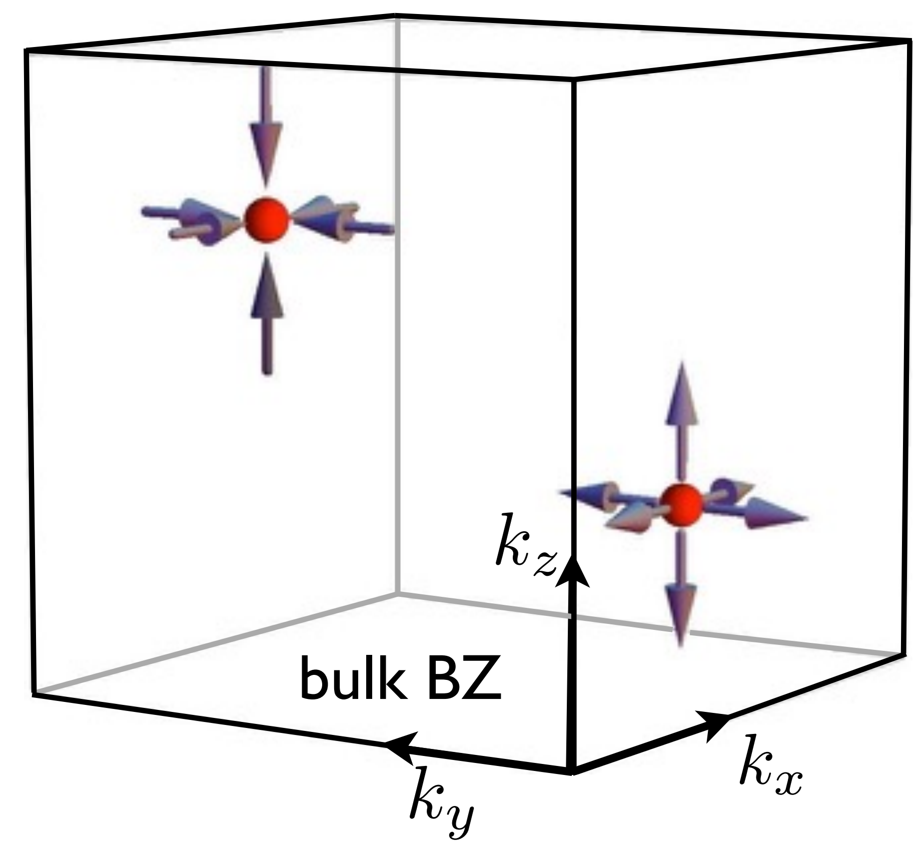

Wan et al., PRB 83, 205101 (2011)

Weyl physics

Touching of two bands in 3D is generically **linear**

$$\hat{H} = \vec{v}_0 \cdot \vec{q}\,\mathbb{1} + \sum_{j=1}^{3} \vec{v}_j \cdot \vec{q}\,\sigma_j$$ **Weyl nodes**

Weyl nodes are **sources/sinks of Berry flux**
with charge/chirality $\mathrm{sign}[\vec{v}_1 \cdot (\vec{v}_2 \times \vec{v}_3)]$

protected surface states: **Fermi arcs**

topological semi-metal with **protected** surface states
(metallic cousin of the topological insulator)

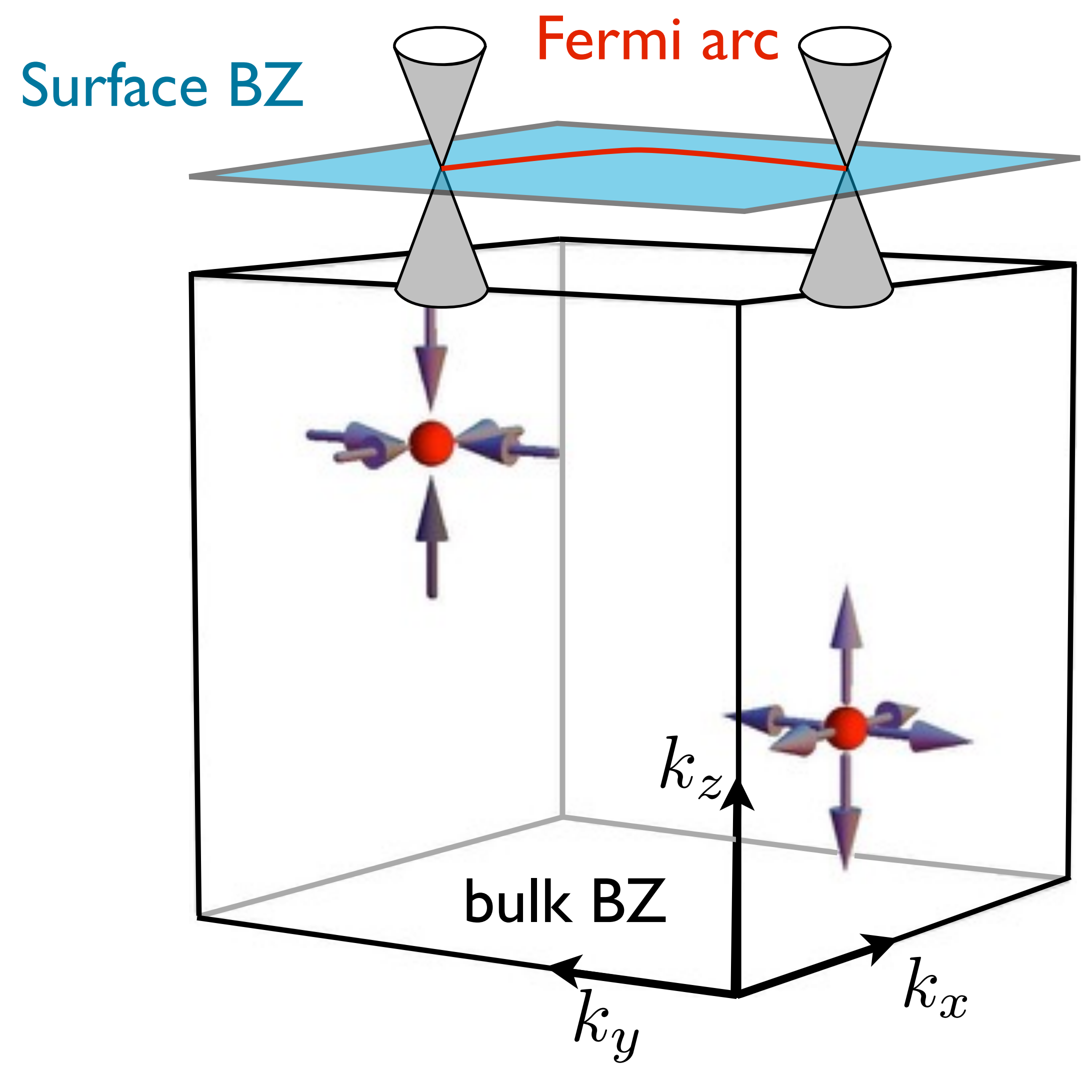

Wan et al., PRB 83, 205101 (2011)

Weyl spin liquids

external **magnetic field** in (1,1,1)-direction

$$H_{eff} = -J \sum_{\langle j,k \rangle} \sigma_j^\gamma \sigma_k^\gamma - \kappa \sum_{\langle j,k,l \rangle} \sigma_j^\alpha \sigma_k^\beta \sigma_l^\gamma$$

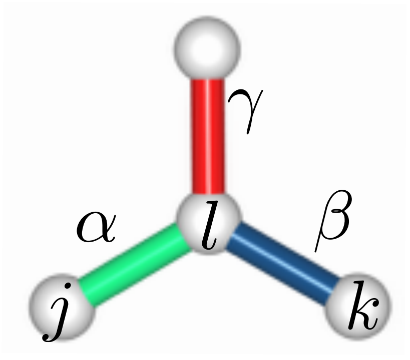

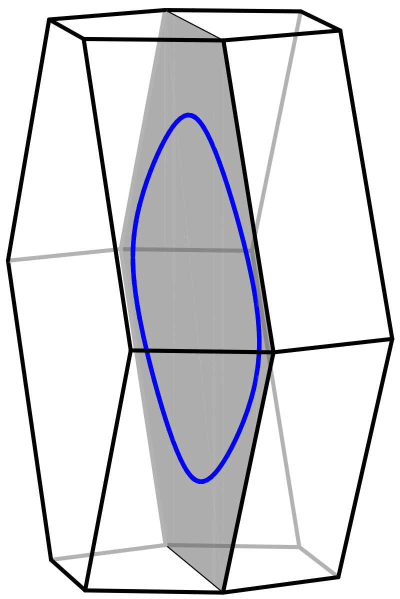

Weyl spin liquids

external **magnetic field** in (1,1,1)-direction

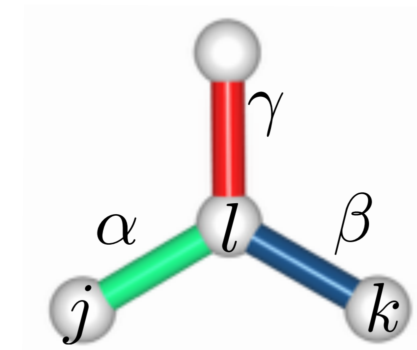

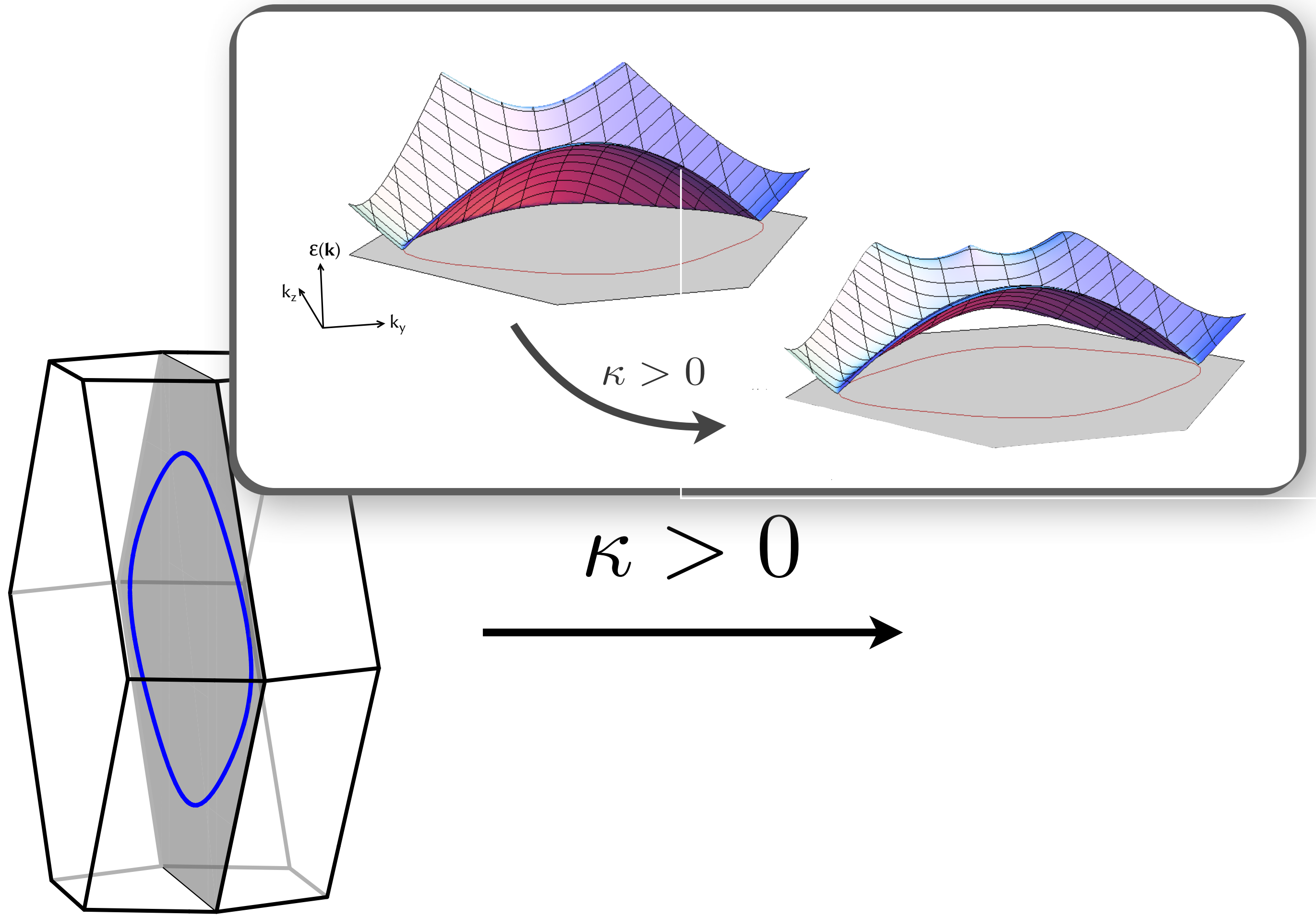

Weyl spin liquids

external **magnetic field** in (1,1,1)-direction

$$H_{eff} = -J \sum_{\langle j,k \rangle} \sigma_j^\gamma \sigma_k^\gamma - \kappa \sum_{\langle j,k,l \rangle} \sigma_j^\alpha \sigma_k^\beta \sigma_l^\gamma$$

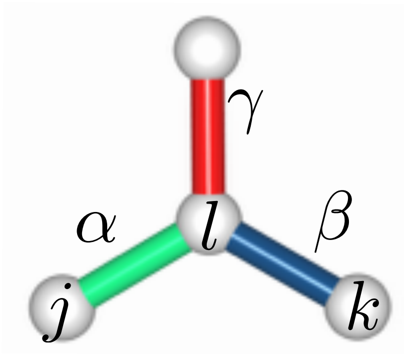

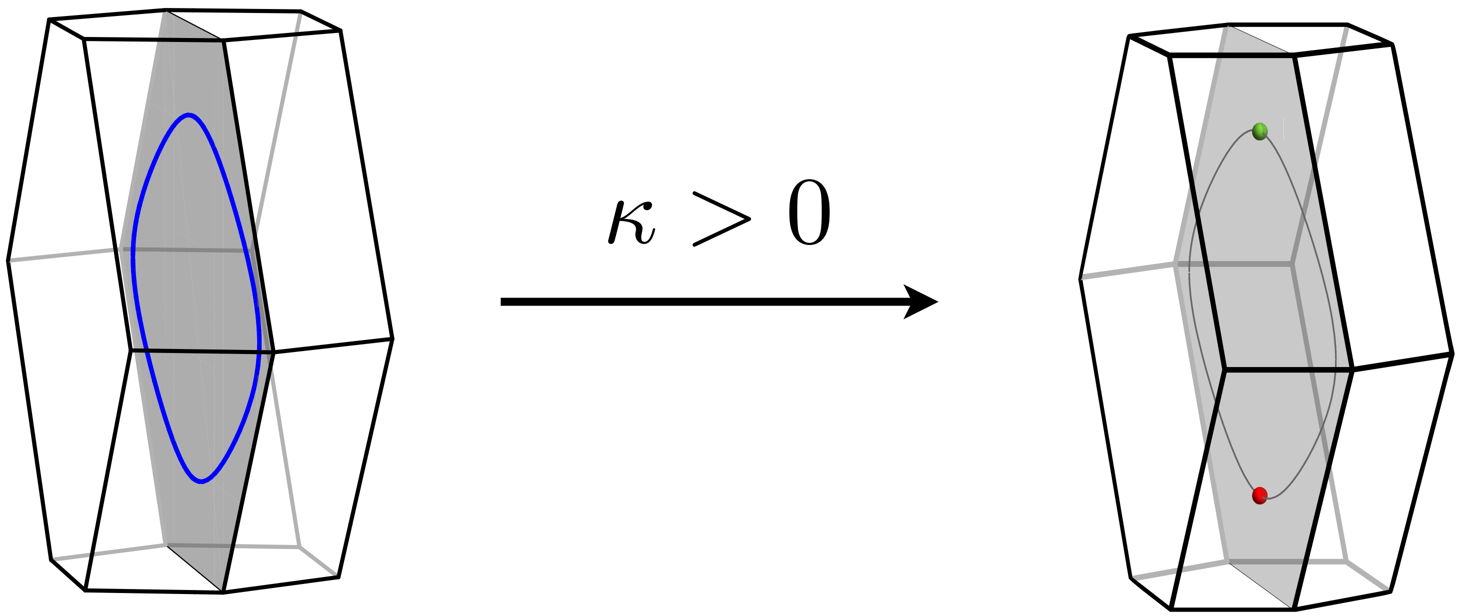

Breaking time-reversal reduces line to a **pair of gapless Weyl nodes**

Weyl nodes are pinned to zero energy due to inversion symmetry

Topology of Weyl spin liquids

Sources/sinks of Berry flux with chirality $\mathrm{sign}[\vec{v}_1 \cdot (\vec{v}_2 \times \vec{v}_3)]$

non-zero Chern number for surface surrounding a Weyl node

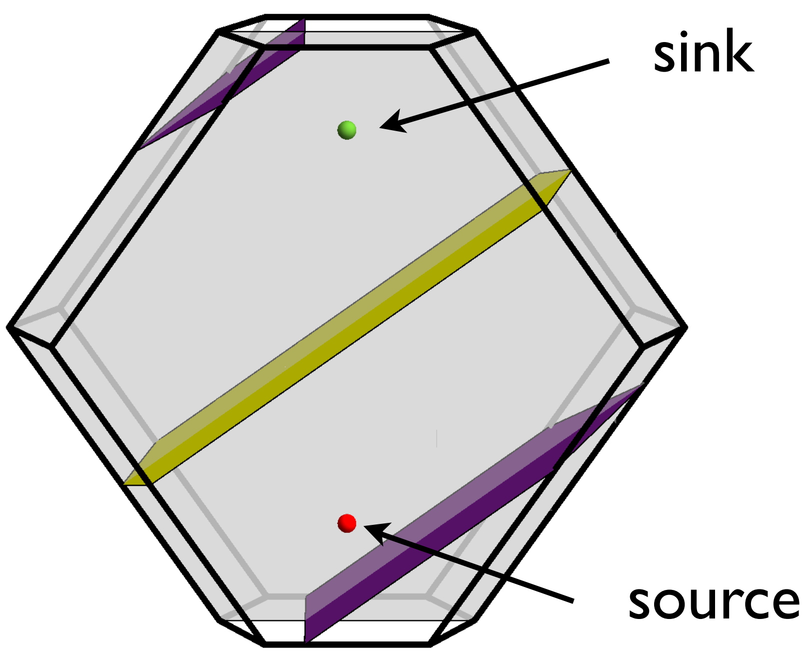

$\kappa = 0.05$

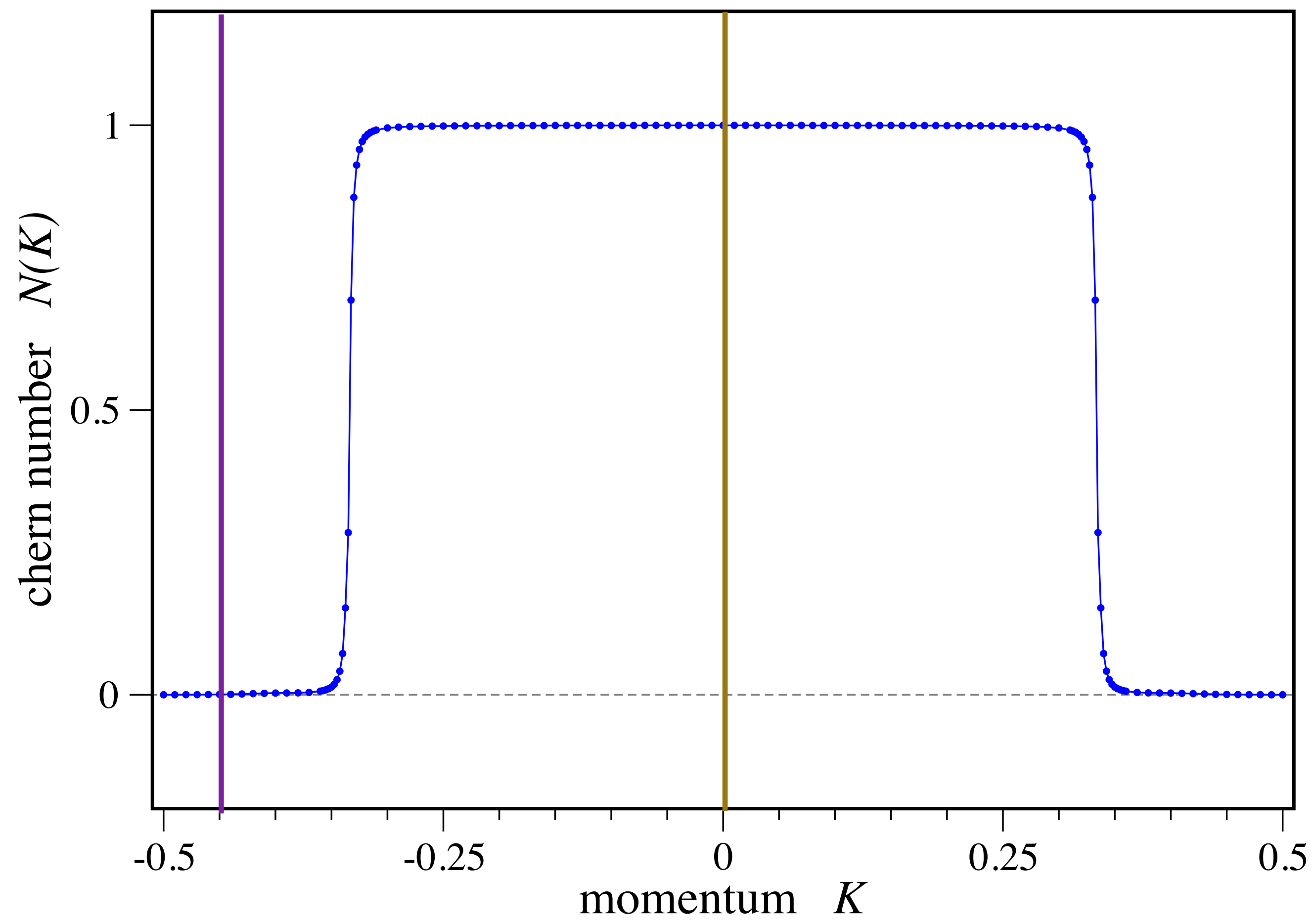

Topological surface states – Fermi arcs

slab geometry

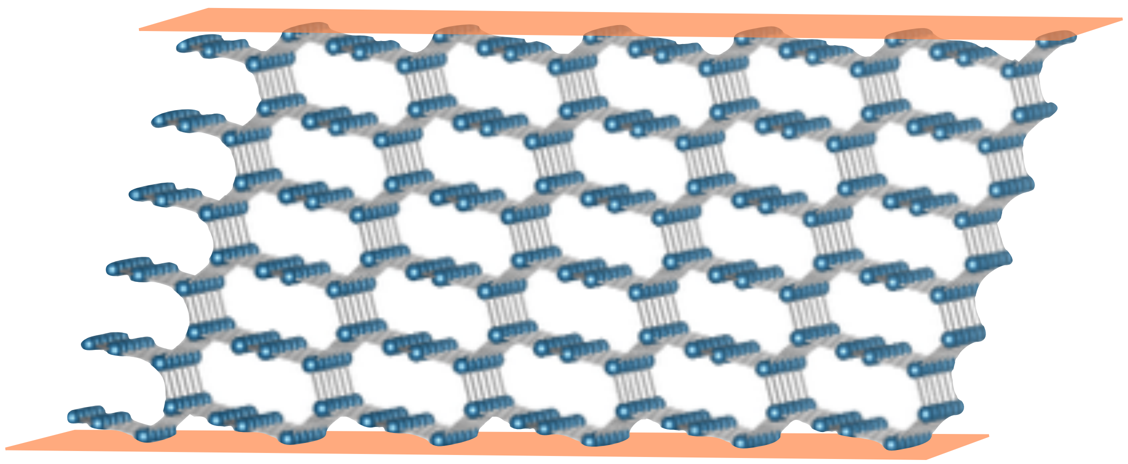

surface Brillouin zone

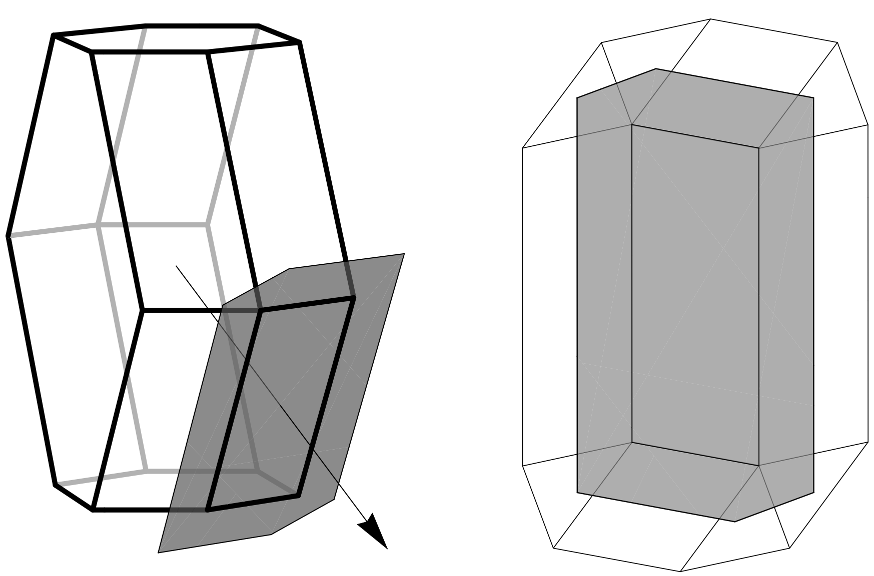

Topological surface states – Fermi arcs

slab geometry

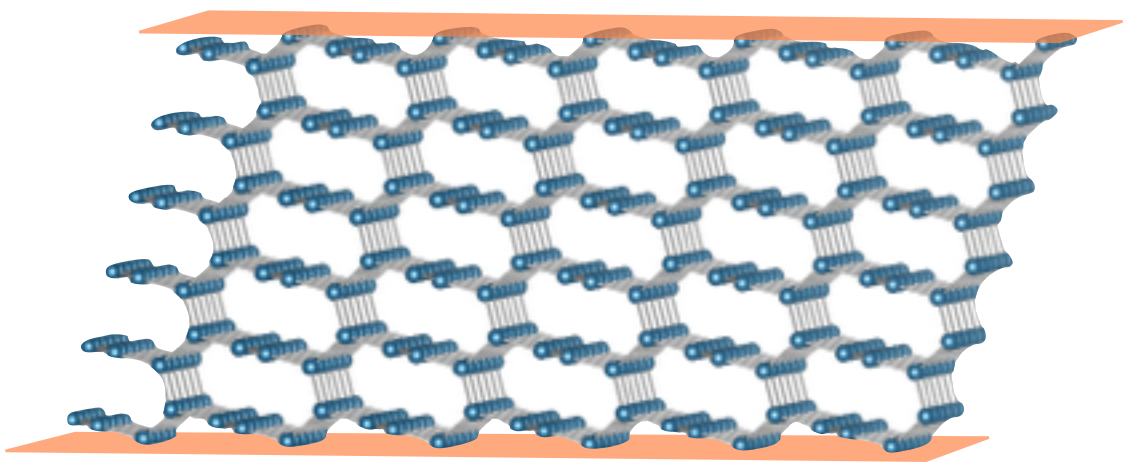

surface Brillouin zone

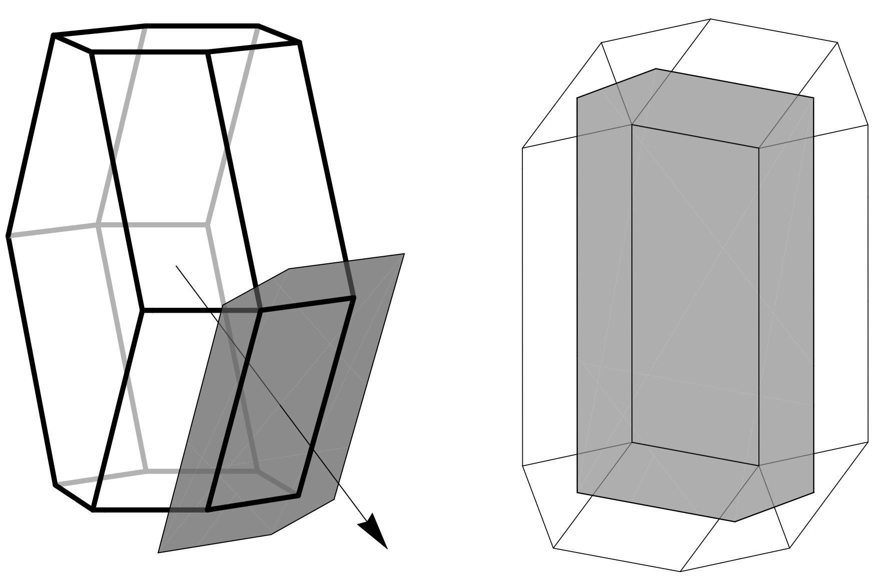

topologically protected gapless surface states

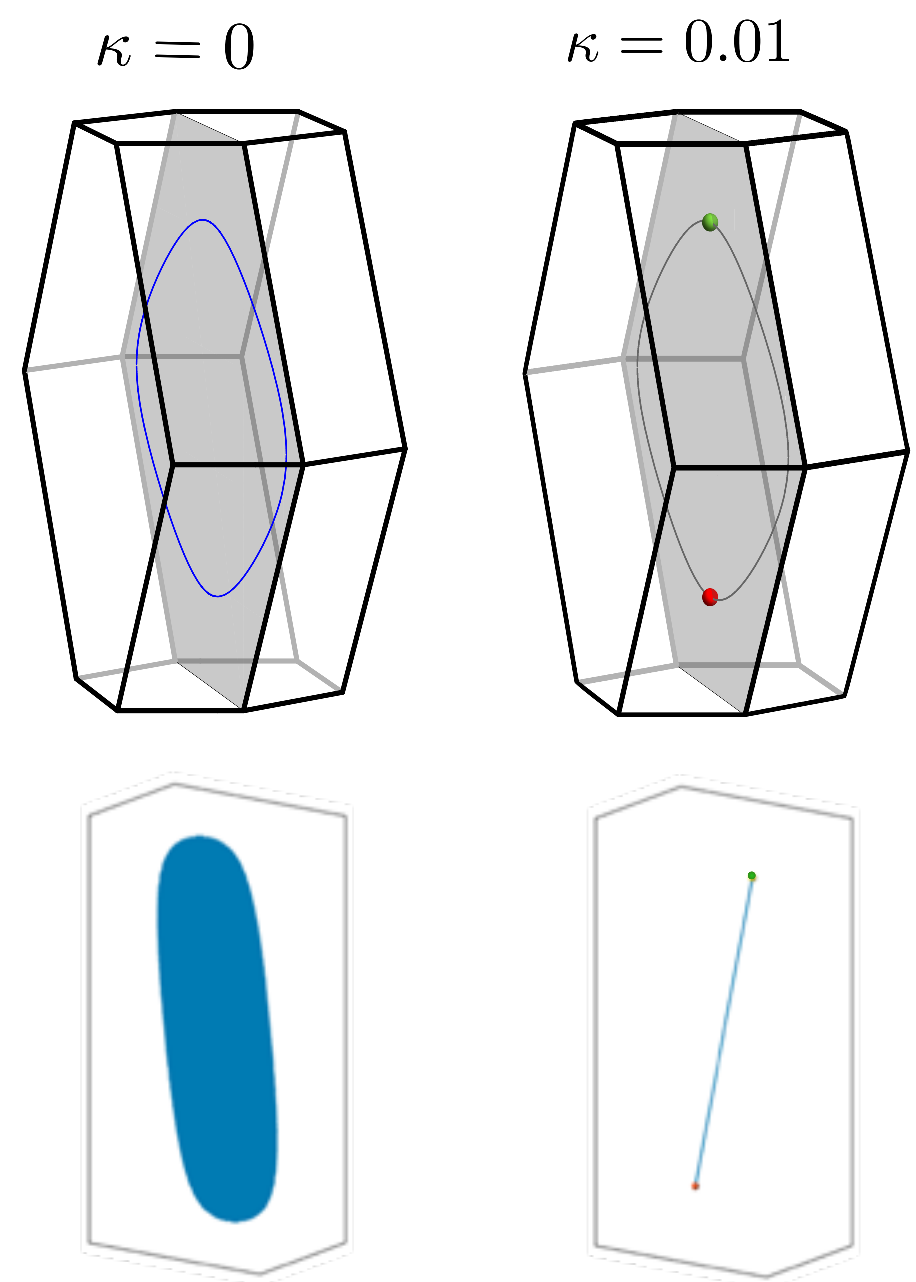

Kitaev models in 3D

Schäfli symbol	Majorana metal	TR breaking	Peierls instability
(10,3)a (hyperoctagon)	(topological) Fermi surface	(topological) Fermi surface	✓
(10,3)b (hyperhoneycomb)	Fermi line	Weyl nodes	✗
(10,3)c	Fermi line	topological Fermi surface	✗
(9,3)a	Weyl nodes	Weyl nodes	✗
(9,3)b	-	-	
(8,3)a	(topological) Fermi surface	(topological) Fermi surface	
(8,3)b	Weyl nodes	Weyl nodes	✓
(8,3)c	Fermi line	Weyl nodes	✗
(8,3)n	gapped	gapped	✗
(6,3)a (honeycomb)	Dirac points	gapped NA	✗

explicit breaking of time-reversal symmetry

Kitaev models in 3D

Schäfli symbol	Majorana metal	TR breaking	Peierls instability
(10,3)a (hyperoctagon)	(topological) Fermi surface	(topological) Fermi surface	✓
(10,3)b	Fermi line	Weyl nodes	✗
	Fermi line	topological Fermi surface	✗
(9,3)a	Weyl nodes	Weyl nodes	✗
(9,3)b	-	-	
(8,3)a	(topological) Fermi surface	(topological) Fermi surface	
(8,3)b	Weyl nodes	Weyl nodes	✓
(8,3)c	Fermi line	Weyl nodes	✗
(8,3)n	gapped	gapped	✗
(6,3)a (honeycomb)	Dirac points	gapped NA	✗

spontaneous breaking of time-reversal symmetry

explicit breaking of time-reversal symmetry

Kitaev models in 3D

Schäfli symbol	Majorana metal	TR breaking	Peierls instability
(10,3)a (hyperoctagon)	(topological) Fermi surface	(topological) Fermi surface	✓
(10,3)b	Fermi line	Weyl nodes	✗
	Fermi line	topological Fermi surface	✗
(9,3)a	Weyl nodes	Weyl nodes	✗
(9,3)b	-	-	
(8,3)a	(topological) Fermi surface	(topological) Fermi surface	
(8,3)b	Weyl nodes	Weyl nodes	✓
(8,3)c	Fermi line	Weyl nodes	✗
(8,3)n	gapped	gapped	✗
	points	gapped NA	✗

spontaneous breaking of time-reversal symmetry

explicit breaking of time-reversal symmetry

Weyl spin liquid with inversion and time-reversal symmetry

Conclusion

- 3D Kitaev models show rich behavior depending on the underlying lattice structure
- Z_2 spin liquid with
  - Majorana Fermi surface
  - Fermi line
  - Weyl nodes (Weyl spin liquid)

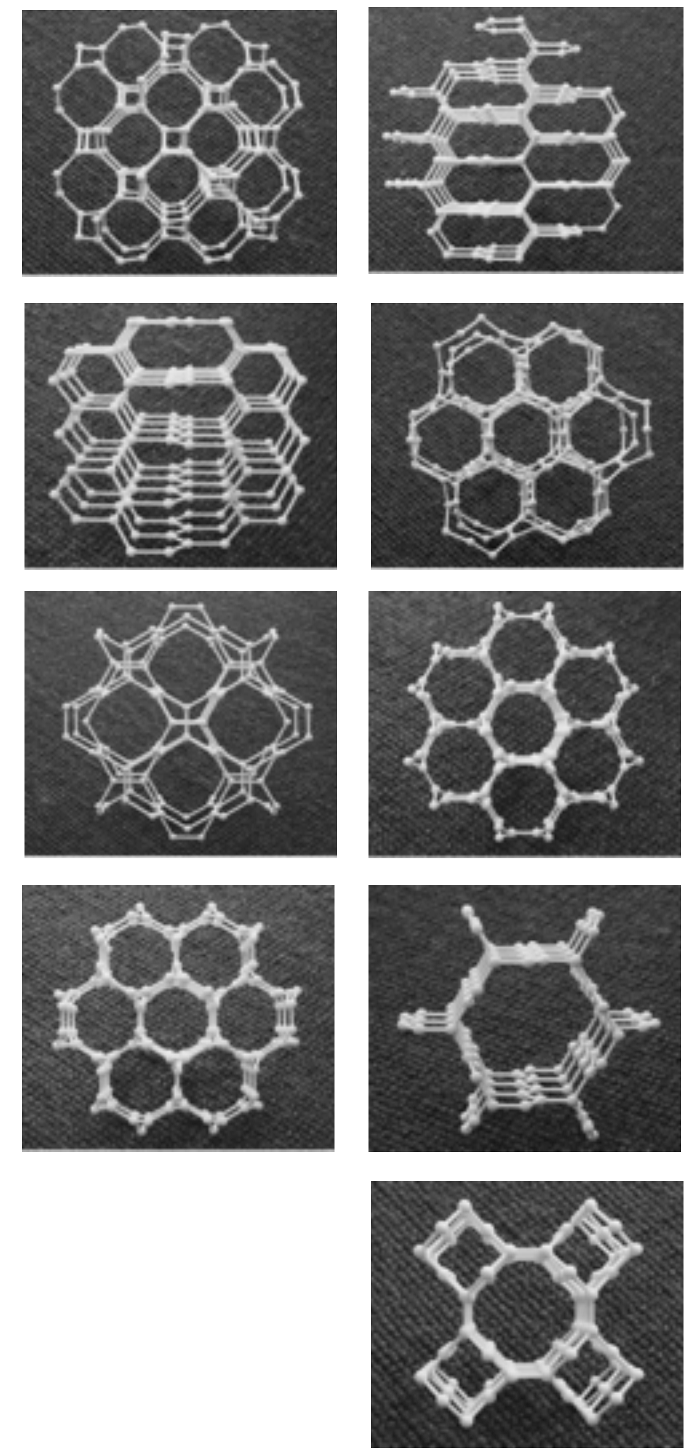

Conclusion

- 3D Kitaev models show rich behavior depending on the underlying lattice structure
- Z_2 spin liquid with
  - Majorana Fermi surface
  - Fermi line
  - Weyl nodes (Weyl spin liquid)

- Can be distinguished experimentally by e.g. specific heat measurements

Fermi surface: $C(T) \propto T$

Fermi line: $C(T) \propto T^2$

Weyl nodes: $C(T) \sim a_{\mathrm{bulk}} \cdot L^3 \cdot T^3 + a_{\mathrm{surf}} \cdot L^2 \cdot T$

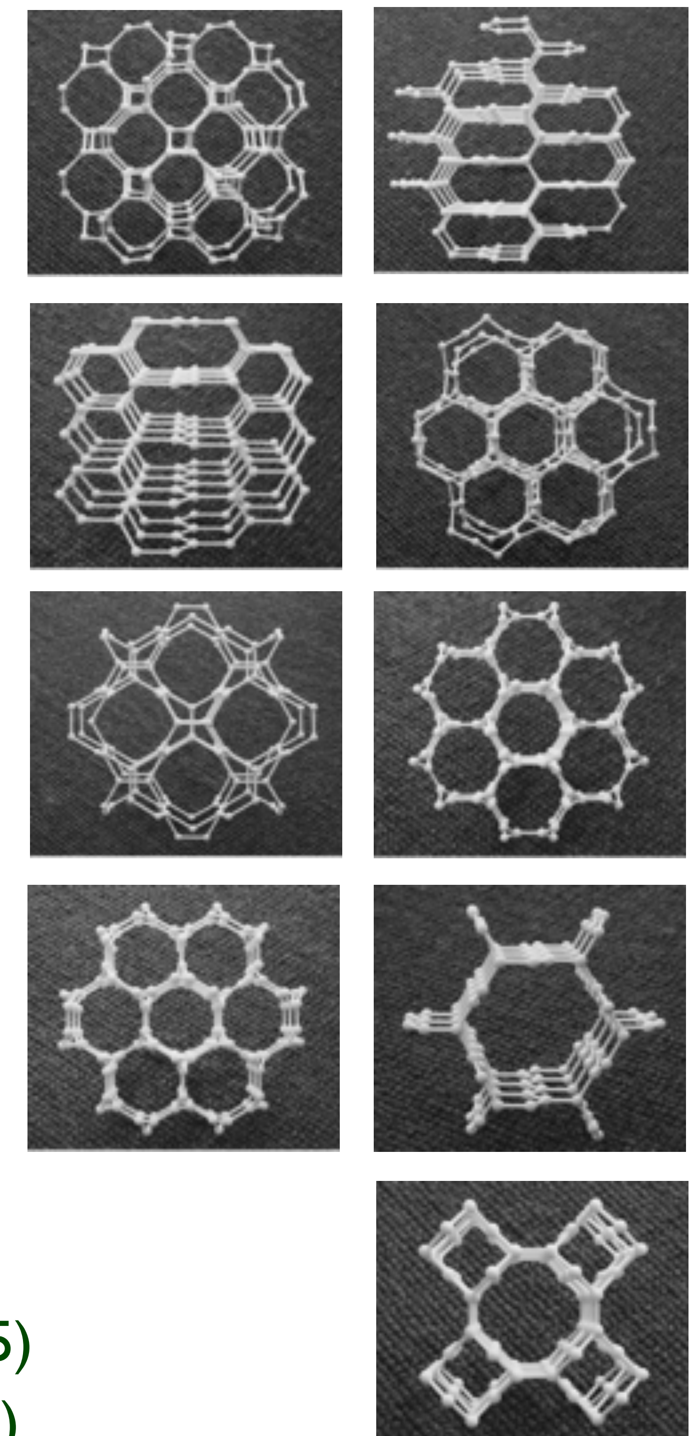

M.H., S. Trebst, PRB 89, 235102 (2014)

M.H., K. O'Brien, S. Trebst, PRL 114, 157202 (2015)

M.H., S. Trebst, A. Rosch, arXiv:1506.01379 (2015)

K. O'Brien, M.H, S. Trebst (in preparation)